Bioorganic Chemistry 127 (2022) 105997

Contents lists available at ScienceDirect

Bioorganic Chemistry

journal homepage: www.elsevier.com/locate/bioorg

Hexa-substituted cyclotriphosphazene derivatives containing hetero-ring chalcones: Synthesis, *in vitro* cytotoxic activity and their DNA damage determination

Asiye Beytur [a], Çiğdem Tekin [b], Eray Çalışkan [c], Suat Tekin [a], Kenan Koran [d,*], Ahmet Orhan Görgülü [e], Süleyman Sandal [a,*]

[a] Physiology Department, Faculty of Medicine, Inonu University, Malatya, Turkey
[b] Department of Health Care Services, Vocational School of Health Services, Inonu University, Malatya, Turkey
[c] Department of Chemistry, Faculty of Arts and Science, Bingol University, Bingöl, Turkey
[d] Department of Chemistry, Faculty of Science, Fırat University, Elazığ, Turkey
[e] Department of Chemistry, Faculty of Science, Marmara University, Istanbul, Turkey

ARTICLE INFO

Keywords:
Cyclotriphosphazene
Cytotoxicity
Genotoxicity
Chalcones
Synthesis

ABSTRACT

In this study, hetero ring hexasubstituted cyclotriphosphazes were obtained in two steps and these compounds were investigated in terms of in vitro cytotoxicity and genotoxicity. The structural characterizations of the starting compounds **1**–**4** were defined by FT-IR, elemental analysis, and NMR (^{1}H and ^{13}C) spectroscopy techniques. In addition to these techniques, the ^{31}P NMR spectroscopy technique was also used in the characterization of cyclotriphosphazenes **(FSC 1–4)**. The changes in cell viability at 1, 5, 25, 50, and 100 μM concentrations against human ovarian (A2780) and human prostate (PC-3 and LNCaP) cell lines for 24 h were determined by the MTT assay method. According to MTT assay results, the inhibitory concentration 50 (IC_{50}/$LogIC_{50}$) value was calculated in Graphpad Prism 6 program. The comet assay was performed to determine whether the effects of compounds on cell viability were through DNA damage. In the comet assay experiments, the highest concentration of compounds (100 μM) was applied to the cells for 24 h and tail length (TL), tail intensity (TI), olive tail moment (OTM) parameters were examined. The results showed that the compound **1**–**4** and **FSC 1**–**4** compounds reduced the cell viability against all cancer cell lines ($p < 0.05$). At the same time, different concentrations of these compounds caused DNA damage in all three cell types ($p < 0.05$). The possible interactions and chemical mechanisms of the synthesized compounds were explained by computational methods with molecular docking. In addition, pharmacological properties of drug candidate molecules have been defined. Experimental and calculated data comply with each other. The study results showed that these compounds have cytotoxic effects against cancer cells and suggested that these effects have occurred through genotoxicity.

1. Introduction

Phosphazenes, which constitute an important class of inorganic chemistry, -[N = PR_2]- can be found in linear, cyclic, or high molecular weight polymeric structures. One of the important members of this group is a six-membered cyclotriphosphazene (Hexachlorocyclotriphosphazene, trimer, $N_3P_3Cl_6$), a six-membered planar ring structure in which nitrogen and phosphorus atoms are sequentially linked to each other. As a result of the substitution reactions of chlorides attached to the phosphorus atom in the cyclotriphosphazene with various nucleophiles, cyclotriphosphazene compounds with different properties can be obtained. Therefore, these compounds are chosen as the main skeleton by researchers [1,2].

Cancer is a disease that occurs as a result of irregular DNA replicating itself and uncontrolled proliferation and growth of cells. It is the second most common disease in the world that causes death. While anticancer drugs are being developed for the treatment of the disease, taking into account the irregular replication of DNA and uncontrolled proliferation and growth of the cells in the disease, molecules that will cause DNA destruction and rapidly kill the dividing cells are tried to be designed. Reported studies show that phosphazene-derived structures have various biological activities ranging from antimicrobial and anti-cancer

* Corresponding authors.
E-mail addresses: kkoran@firat.edu.tr (K. Koran), suleyman.sandal@inonu.edu.tr (S. Sandal).

https://doi.org/10.1016/j.bioorg.2022.105997
Received 12 March 2022; Received in revised form 9 June 2022; Accepted 27 June 2022
Available online 30 June 2022

activity to inhibit the growth of cancer cells by breaking down DNA [3–5]. For this purpose, studies are still ongoing to obtain new bioactive compound derivatives by combining different bioactive compounds over the main skeleton of phosphazene [6–15].

Flavonoids constitute the most important and broadest class of natural bioactive products derived from plants, and the most known subclass of are chalcones, also called "open chain flavonoids" [16]. Chalcones are used in traditional medicine to treat many diseases [17]. Two aromatic rings chemically linked to each other by the enon system constitute the basic skeletal structure of chalcones [18]. Numerous synthesis methods have been reported in the literature for the synthesis of chalcone derivatives. Among these, the most preferred synthesis method is Claisen-Schmidt condensation, but Suzuki, cross-coupling, Heck, Friedel-Crafts and Julia-Kocienski reactions are also known and used in the literature [19,20]. Chalcones and their synthetic derivatives have a wide spectrum of bioactivity such as anti-hypertensive, anti-diabetic, anti-retroviral, anti-histamine, anti-inflammatory, anti-oxidant, anti-tuberculosis, anti-fungal, anti-ulcer, and anticancer [17,21–24]. There are many studies in the literature on the investigation of biological properties of chalcone derivatives. However, despite the wide range of biological properties, these compounds have demonstrated, it is clear that there is still a need to synthesize new derivatives. In this context, three important strategies are followed information of new chalcone derivatives that tend to show anticancer activity. These are replacing aromatic rings with heteroaromatic rings, making various substitutions in aromatic rings, and forming a hybrid chalcone with another molecule showing anticancer activity [25].

This study demonstrated that new chalcone derivatives were obtained by four of the heterocyclic aldehydes that have an important role in medicinal chemistry research which are 1-methyl-1*H*-imidazole-2-carbaldehyde, 6-methoxynicotinaldehyde, fluorene-2-carboxaldehyde and 2,3-dihydrobenzofuran-5-carbaldehyde reacted with 4′-hydroxy acetophenone by following the Claisen-Schmidt condensation [20,26]. Hexa substituted cyclotriphosphazene derivatives were obtained as a result of the reaction of the chalcone compounds obtained in the previous step with hexachlorocyclotriphosphazene and the structural characterization of the compounds was performed using elemental analysis, ^{1}H, ^{13}C and ^{31}P NMR spectroscopic methods, respectively. In vitro cytotoxicity activities of pure compounds were determined by MTT assay method using human ovarian cancer (A2780) and human prostate cancer (PC-3 and LNCaP) cell lines at 1, 5, 25, 50 and 100 μM doses. The possible interactions and chemical mechanisms of the synthesized compounds were explained by computational methods with molecular docking. Significant reductions in cell viability were observed in all cells, especially at high doses, and the DNA damage analysis at the dose at which the compounds showed the best effect was performed by the Comet Assay method. Comet analysis results showed that changes were observed in tail lenght (TL), tail intensity (TI), olive tail moment (OTM) parameters and these changes were statistically significant. As a result, cell death proceeds through the DNA damage mechanism.

2. Results and discussion

2.1. Chemistry

Hexa-substituted cyclotriphosphazenes (**FSC 1–4**) were prepared by the reaction of hexachlorocyclotriphoshazene **(FSC)** with hetero ring chalcone compounds **1–4**. General synthetic route and their numbering for ^{1}H, and ^{13}C NMR characterizations for compounds **1–4** is given in Scheme 1.

The single peak in the spectra of compounds **FSC 1–4** shows that the chemical environment of the phosphors in the structure is the same and has a symmetrical structure. It is seen that the spin system is in the form of A3. The phosphazene compounds and their numbering for ^{31}P, ^{1}H, and ^{13}C NMR characterizations is shown in Scheme 2. As the ^{31}P NMR spectrum was examined, the peak belonging to hexachlorocyclotriphosphazene **(FSC)** and equivalent phosphors observed at approximately 21.12 ppm was not observed in the ^{31}P NMR spectrum of **FSC 1–4** compounds. In addition, the phosphorus peak shifted to the high area with the effect of the substituent attached to the phosphazene ring. This means that the electron density of the phosphorus atom increases. This is because the electrons in the P=N bond concentrate on the phosphorus as a result of the electron withdrawal of the substituent attached to the phosphazene ring.

When the proton NMR spectrum of hexasubstituted structures were examined, it was not observed that the –OH proton in the structure of compounds **1–4** was replaced by the chlorine atom in the phosphorus atom. This situation is an important indicator that the structure is bonded. In addition, it is seen that the integral heights are compatible with the structure. The structures of compounds were verified by ^{31}P, ^{1}H, ^{13}C NMR, and FT-IR analyses. ^{31}P, ^{1}H, and ^{13}C NMR spectra of the compound **FSC-1** are given in Fig. 1.

The first evidence that the chalcone compound is bound to the hexachlorocyclotriphosphazene compound is understood by the FT-IR spectrum. In this spectrum, instead of –P-Cl bonds, –OH bond in chalcone forms P—O—Ph bond with phosphorus and the values of P—O—Ph stretching vibrations are clearly seen in the spectrum. Relevant data are indicated in the Experimental Section. The second evidence showing the formation of the structure is the ^{31}P NMR spectrum and the ^{31}P NMR value of the Hexachlorocyclotriphosphazene compound resonated as a singlet peak around 21 ppm. For the result of binding to be a singlet peak, it must be either tri-substituted (single chalcone bonding to each

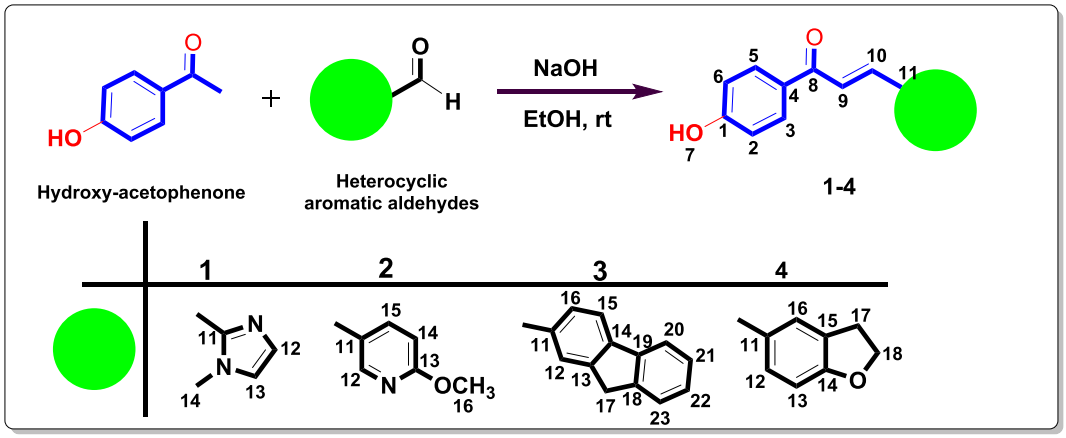

Scheme 1. General synthetic route and their numbering for NMR characterizations for **1–4**. Reaction times and yields: 10 h., 55% yield for compound **1**; 10 h. 65% yield for compound **2**; 10 h. 63% yield for compound **3**; 10 h. 72% yield for compound **4**.

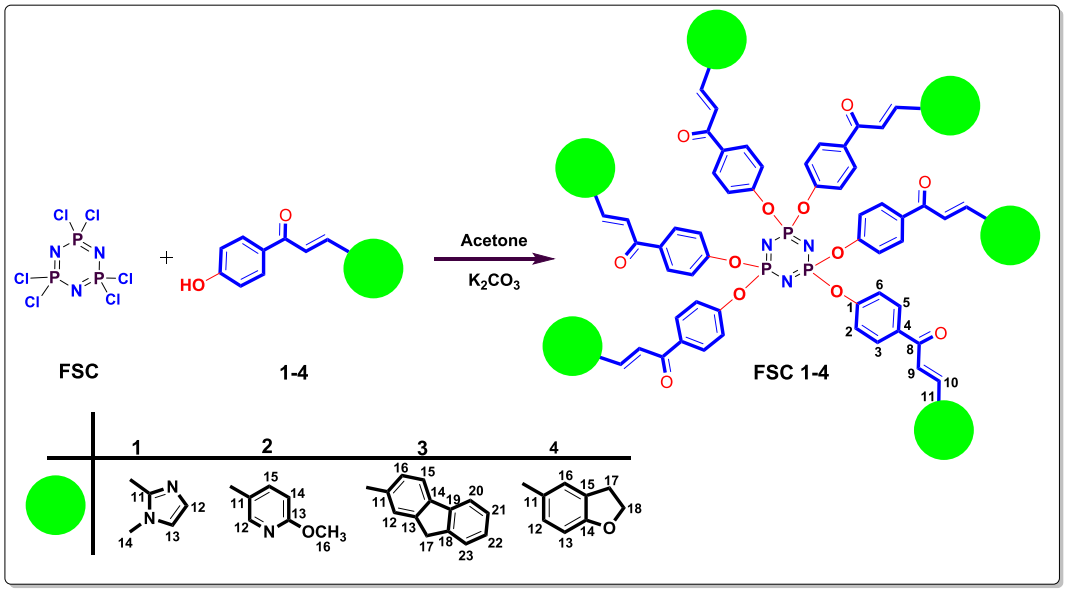

Scheme 2. General Synthetic route for full substituted cyclotriphosphazene compounds **(FSC 1–4).** Reaction times and yields: 8 h., 85% yield for **FSC-1**; 10 h. 82% yield for **FSC-2**; 15 h. 50% yield for **FSC-3**; 15 h. 50% yield for **FSC-4**.

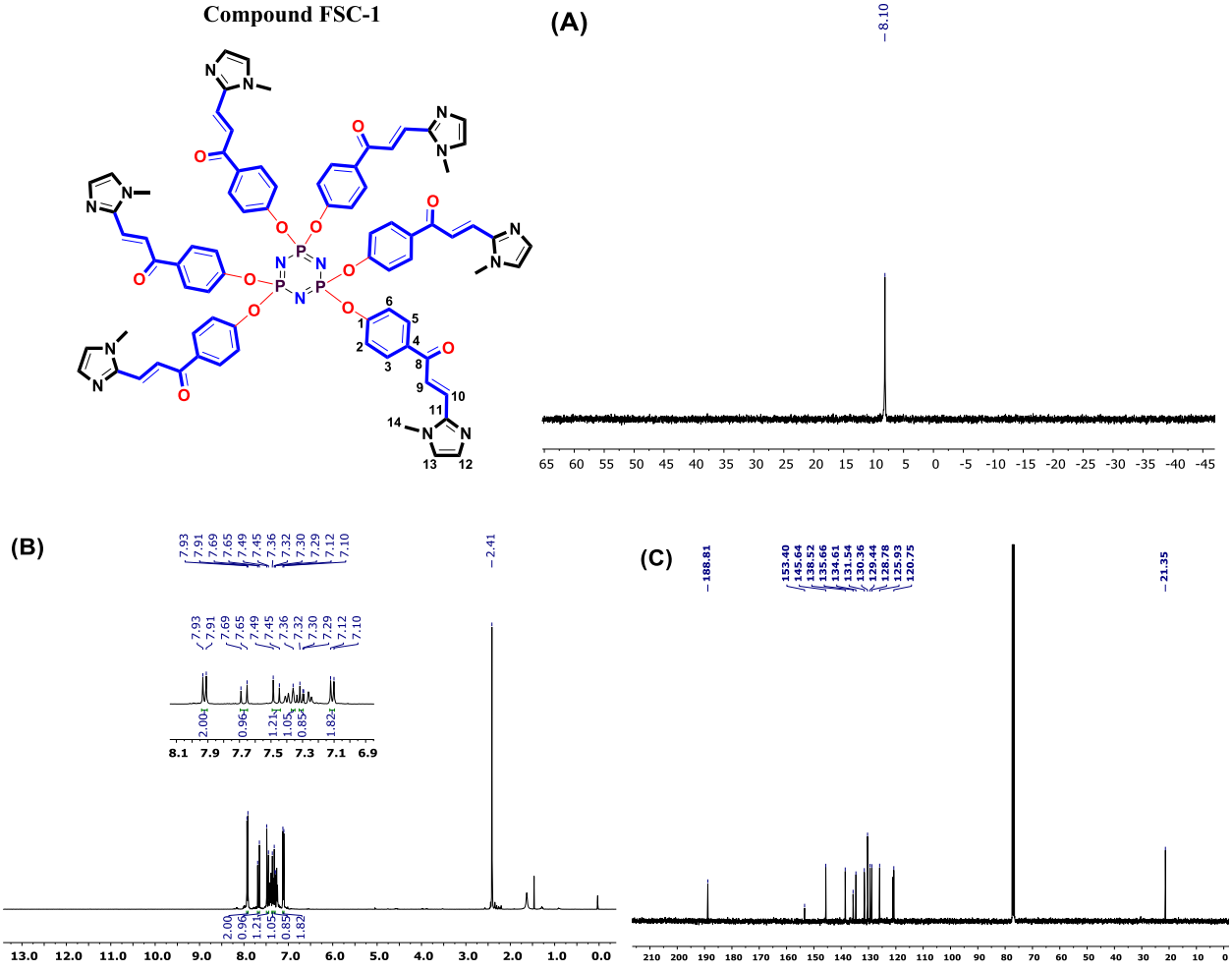

Fig. 1. ^{1}H, ^{13}C and ^{31}P NMR spectrum of compound **FSC-1** (in $CDCl_3$).

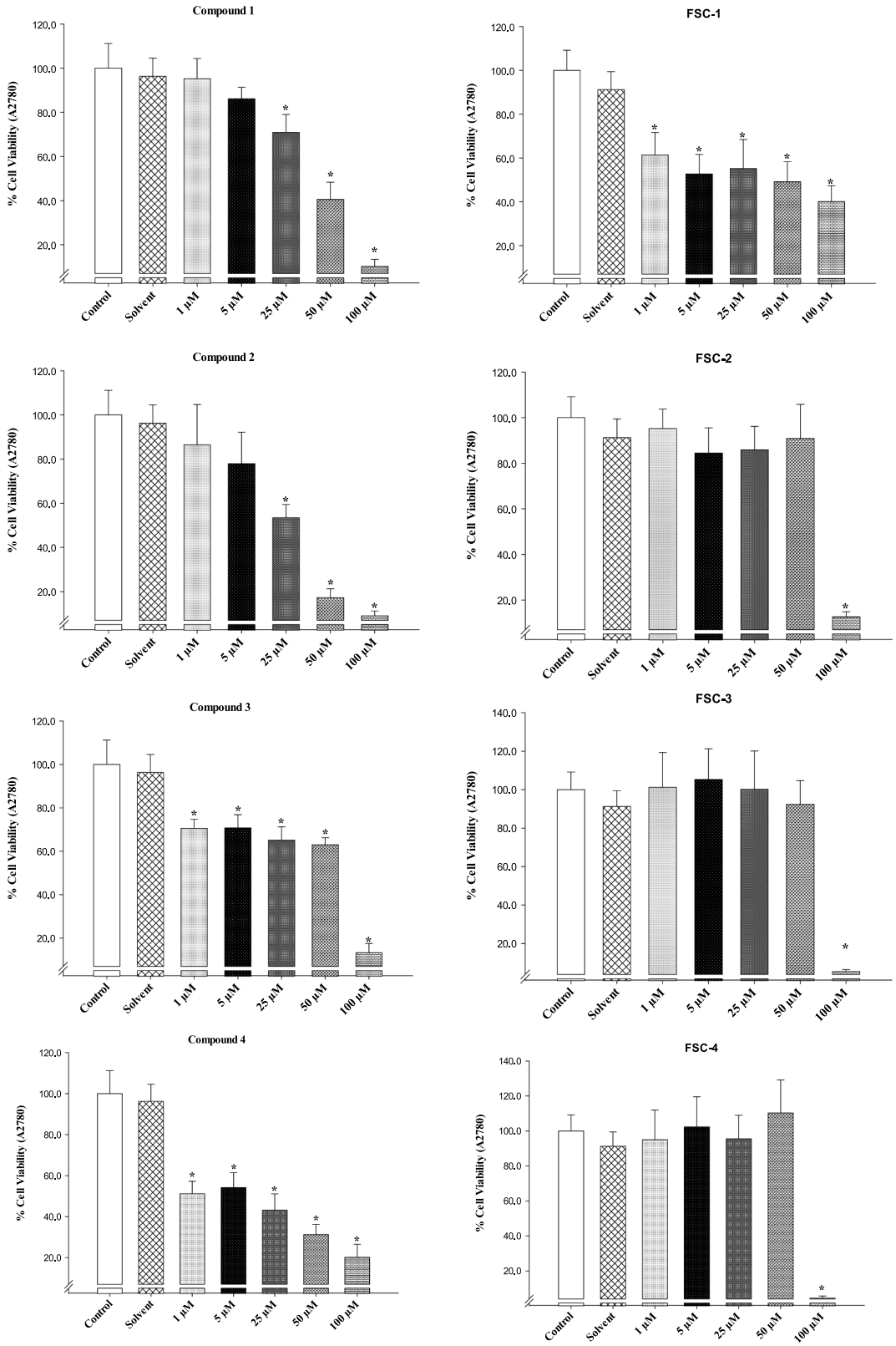

Fig. 2. The relative cell viability (%) of A2780 cells after a 24-h treatment with all the compounds **1**–**4** and **FSC 1**–**4**. The changes on the cell viability (%) caused by compounds are compared with the control data. Each data point is an average of 10 viability (*$p < 0.05$).

phosphorus atom) or hexa-substituted. Supporting evidence of hexa-binding is the elemental analysis and newly added MS results. Along with these, the ^{1}H and ^{13}C NMR spectra support the structure and the melting points appearing as one is the proof that the structure was formed in a pure form. All the characterization spectra of compounds were given in supplementary information (Figs. S1-28).

2.2. Biological evaluation

2.2.1. In vitro cytotoxic activity

Human cancer cell lines (A2780, LNCaP, and PC3) were incubated for 24 h with different concentrations of compounds **1**–**4** and **FSC 1**–**4** (1, 5, 25, 50, and 100 μM) and then % cell viability changes were determined by MTT assay. LogIC_{50}/IC_{50} values were calculated with

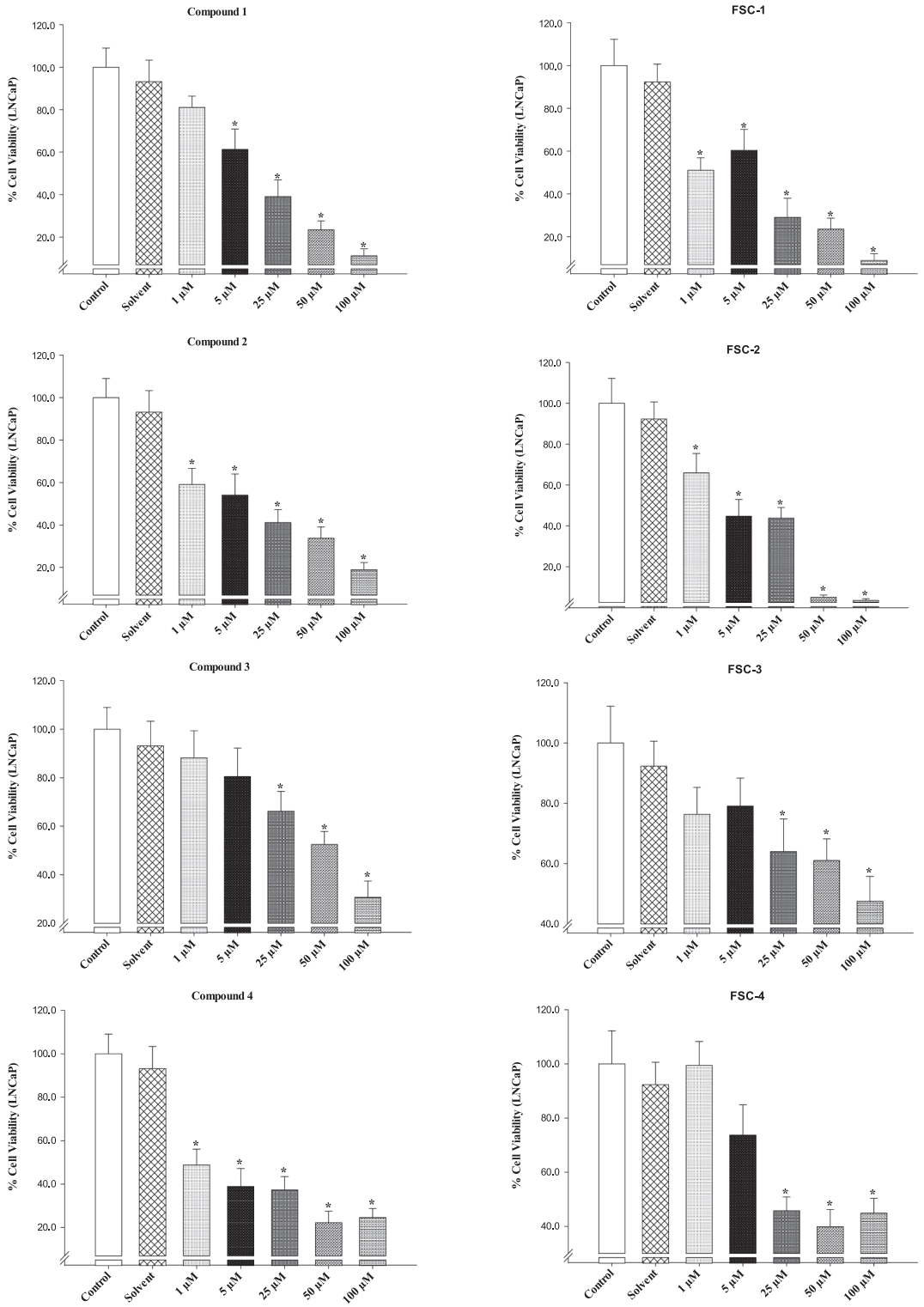

Fig. 3. The relative cell viability (%) of LNCaP cells after a 24-h treatment with all the compounds **1**–**4** and **FSC 1**–**4**. The changes on the cell viability (%) caused by compounds are compared with the control data. Each data point is an average of 10 viability (*$p < 0.05$).

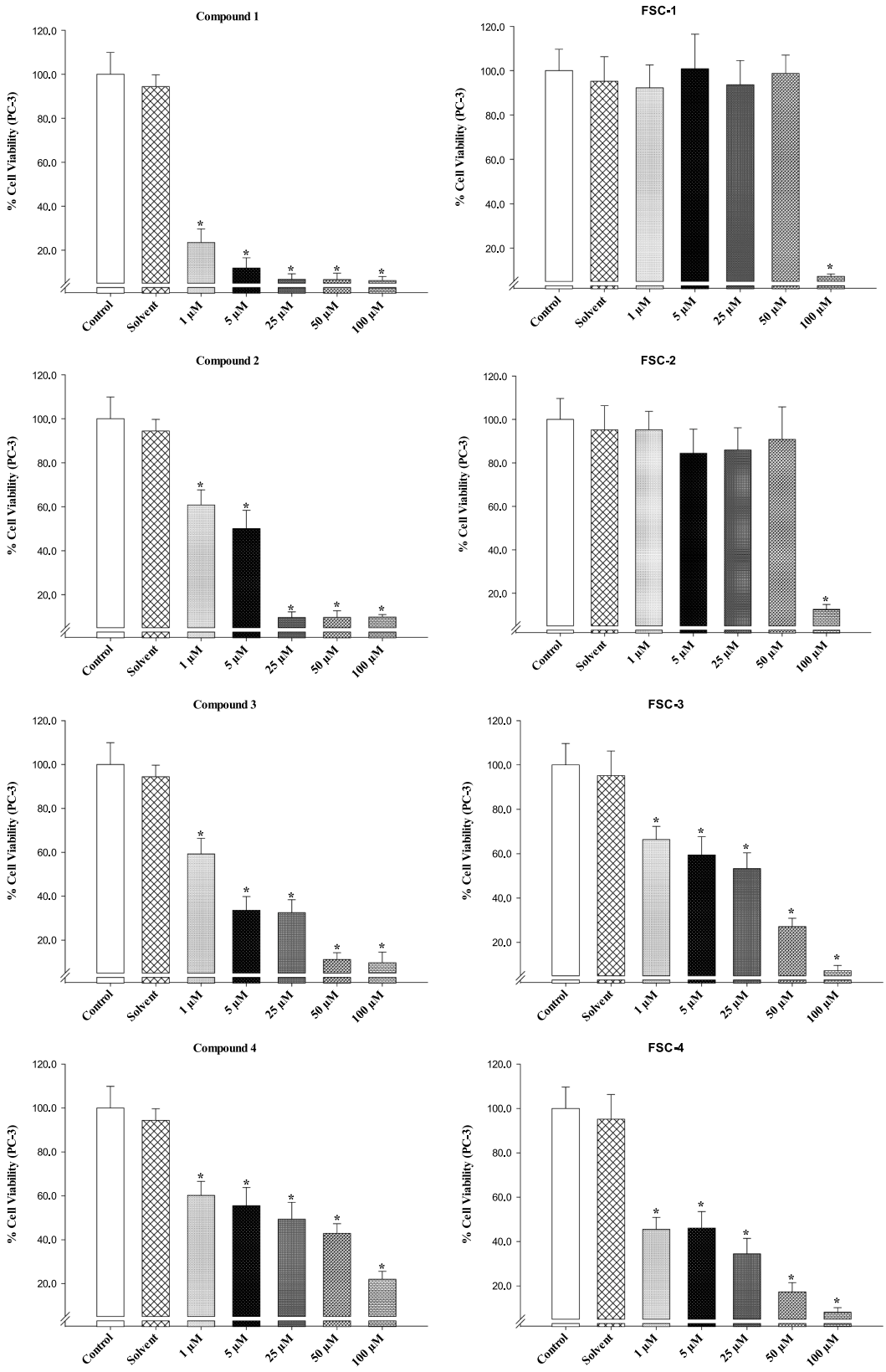

Fig. 4. The relative cell viability (%) of PC-3 cells after a 24-h treatment with all the compounds **1**–**4** and **FSC 1**–**4**. The changes on the cell viability (%) caused by compounds are compared with the control data. Each data point is an average of 10 viability (*$p < 0.05$).

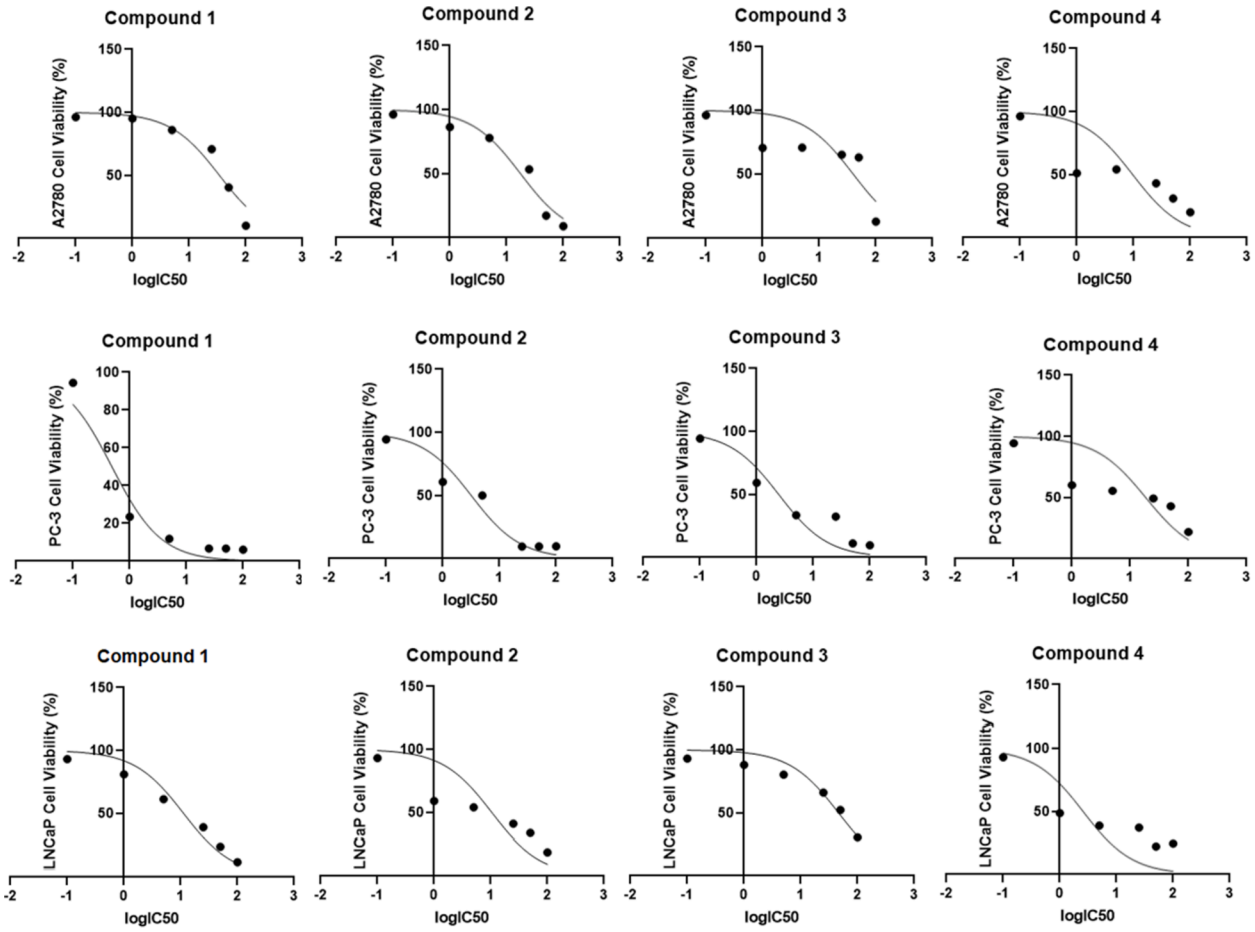

Fig. 5. The $LogIC_{50}$ values against A2780, PC-3 and LNCaP cell viability (%) of compounds **1**–**4**.

Graphpad prism 6 computer program. The related results and graphics are shown in Tables S1-3 and Figs. 2-4. The graph showing the $LogIC_{50}$/IC_{50} values of the compounds are given in Figs. 5 and 6.

The majority of the compounds against A2780 cells significantly reduce the cell viability, especially at 50 and 100 μM doses, and this reduction is also statistically significant ($p^*<0.05$, Fig. 2). On the other hand, compound **3**, compounds **4**, and compound **FSC-1** decreased cell viability in a dose-dependent manner at all doses, and this reduction was also statistically significant ($p^*<0.05$, Fig. 2).

The cell viability results against LNCaP cells of all compounds exhibit a significant effect. Among the tested compounds, especially **FSC-2** was effective at all doses, while it was the compound that showed the most effect at high concentrations (50 and 100 μM).

Cyclotriphosphazene derivatives containing different substituted organic groups have been synthesized and various biological activity studies of these compounds have been carried out [6–11,27–30]. In a study by İbişoğlu *et al.*, the antimicrobial activity of benzimidazole substituted cyclotriphosphazene compounds was tested and it was observed that they were effective against *B. subtilis* [11]. In another study, hydroxyanthraquinone substituted cyclotriphosphazenes compounds were synthesized by Çiftçi et al. and tested against various cancer cells by MTT assay method. The results of this study showed that some compounds were effective on different cancer cells [31]. In different studies conducted by our group, cytotoxicity studies of cyclotriphosphazenes with different chalcone groups were performed against cancer cell lines such as human breast, prostate, and ovarian, and the results showed that several derivatives gave promising results [32–34]. Compared to the cytotoxic activity of the chalcone-substituted cyclotriphosphazenes containing methoxy, methyl, fluorine, and chlorine, which were used in our previous works, the heterocyclic chalcone substituted cyclotriphosphazenes synthesized in this study were more effective against similar human cancer cell lines, especially at low concentrations.

2.2.2. In vitro genotoxicity (DNA damage) properties

Cancer, simply expressed as abnormal growth of cells is one of the leading causes of death in the world. Although significant progress has been made in the diagnosis and treatment of cancer in recent years, the search for new drugs candidates with increased efficacy and minimal side effects still continues intensively. In this regard, chalcones and phosphazene derivatives in particular have attracted great interest because of their potential as anti-cancer agents [35,36]. One of the possible hypotheses put forward is that the majority of the anticancer drugs used in the clinic exert their effects through inhibition of DNA-bound proteins/enzymes or by interacting with DNA directly [37]. It has been suggested as a result of compound − DNA interaction studies that phosphazenes have DNA binding abilities [38]. In addition, it has been reported that aziridine-crown substituted cyclotriphosphazenes, known as hazardous compounds, cleave the DNA and halt the growth of cancer cells [3]. In another study has been shown that new phosphazenes bearing secondary amino and pendant (4-fluorobenzyl) spiro groups were very effective in changing the mobility and unwinding behavior of pBR322 plasmid DNA [35]. In the current study, we synthesized new heterocyclic chalcone compounds and their hexasubstituted phosphazene derivatives and, we tried to determine whether the cytotoxic effects of these substances on prostate and ovarian cancer cell lines are through DNA damage. While compounds **1**–**4** and **FSC 1**–**4** at 100 μM concentration caused statistically significant increases in TI, TL,

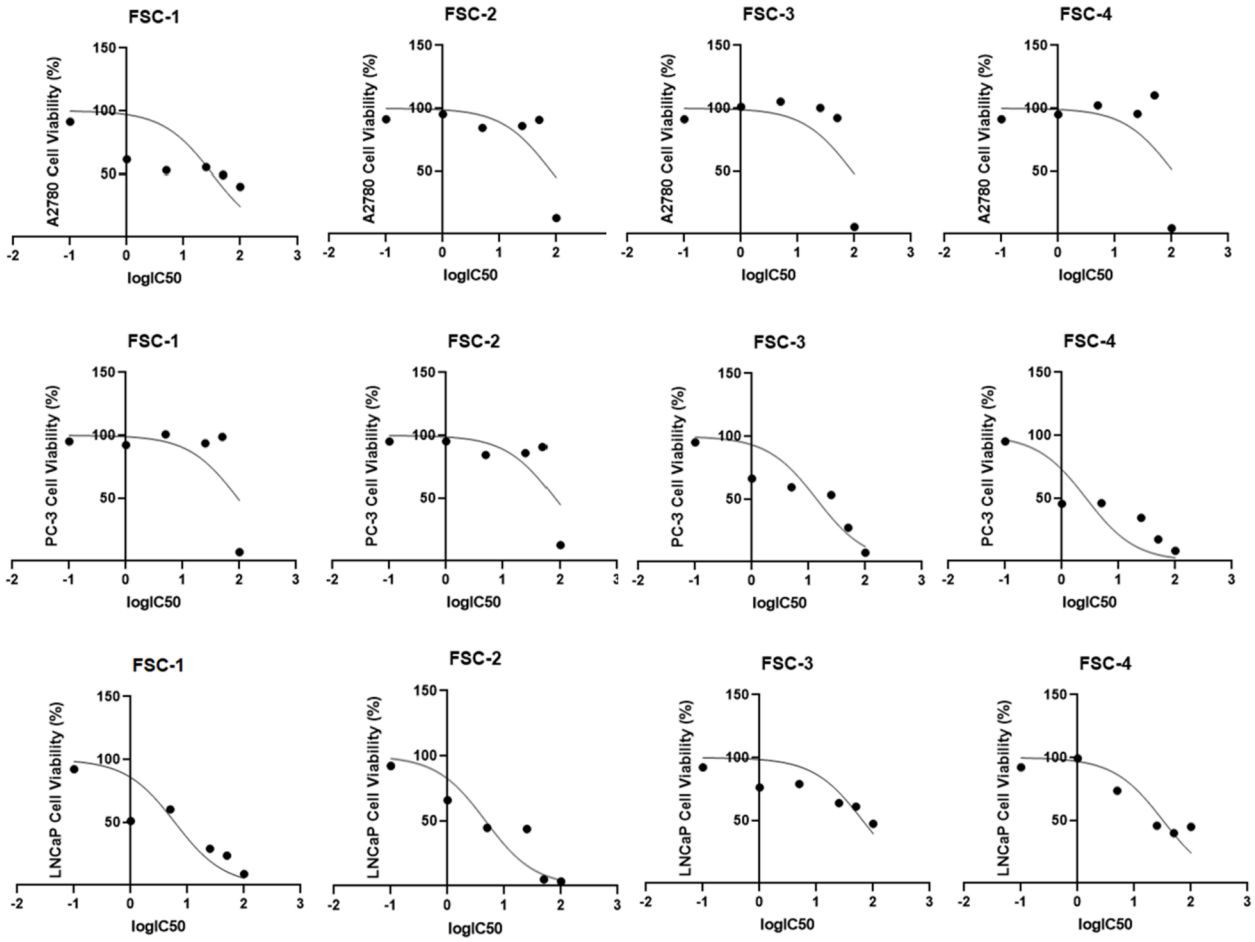

Fig. 6. The $LogIC_{50}$ values against A2780, PC-3 and LNCaP cell viability (%) of **FSC 1**–**4**.

Table 1
DNA damage results in TL, TI, and OTI values 24 h after application of compounds to A2780, LNCaP and PC-3 human cell line cultures (p*<0.05).

		PC-3			LNCAP	
Entry	*Tail Lenght (TL)*	*Tail Intensity (TI)*	*Olive Tail Moment (OTM)*	*Tail Lenght (TL)*	*Tail Intensity (TI)*	*Olive Tail Moment (OTM)*
Control	3,42 ± 0,61	34,30 ± 5,17	0,44 ± 0,08	3,27 ± 0,42	45,33 ± 10,34	0,49 ± 0,12
Solvent	3,43 ± 0,99	39,53 ± 11,43	0,49 ± 0,15	3,61 ± 0,71	36,26 ± 9,36	0,43 ± 0,10
Comp. 1	4,76 ± 0,77*	68,01 ± 15,11*	0,82 ± 0,20*	8,97 ± 1,53*	120,45 ± 18,25*	1,70 ± 0,23*
Comp. 2	4,37 ± 0,58*	61,08 ± 13,15*	0,70 ± 0,14*	6,80 ± 0,81*	91,91 ± 9,31*	1,24 ± 0,17*
Comp. 3	11,19 ± 2,43*	112,91 ± 32,29*	1,59 ± 0,45*	26,97 ± 5,26*	310,13 ± 49,59*	5,27 ± 1,44*
Comp. 4	8,75 ± 1,00*	111,54 ± 10,02*	1,47 ± 0,09*	3,27 ± 0,34	30,54 ± 3,75	0,40 ± 0,05
FSC-1	8,07 ± 1,09*	99,72 ± 9,57*	1,50 ± 0,17*	4,09 ± 0,34*	42,79 ± 7,00	0,54 ± 0,06
FSC-2	4,51 ± 1,33*	50,78 ± 10,58*	0,59 ± 0,14	4,12 ± 1,29	37,67 ± 13,44	0,53 ± 0,19
FSC-3	5,60 ± 1,40*	70,59 ± 11,48*	0,94 ± 0,14*	5,41 ± 1,79*	47,66 ± 11,47	0,69 ± 0,18*
FSC-4	2,88 ± 0,54	27,89 ± 5,16*	0,35 ± 0,08*	3,65 ± 1,16	38,79 ± 9,07	0,53 ± 0,13

		A2780	
Entry	*Tail Lenght (TL)*	*Tail Intensity (TI)*	*Olive Tail Moment (OTM)*
Control	1,46±0,19	8,43±3,17	0,12±0,04
Solvent	1,53±0,37	9,01±4,86	0,14±0,07
Comp. 1	3,08±0,52*	26,73±6,66*	0,44±0,12*
Comp. 2	2,45±0,38*	26,98±4,15*	0,41±0,08*
Comp. 3	9,82±2,33*	119,70±22,94*	2,74±0,43*
Comp. 4	3,57±0,66*	28,81±4,86*	0,52±0,13*
FSC-1	2,67±0,63*	25,70±4,90*	0,37±0,08*
FSC-2	4,96±1,13*	53,46±11,09*	0,94±0,18*
FSC-3	2,45±0,49*	11,98±2,79	0,32±0,10*
FSC-4	2,45±0,49*	24,63±5,64*	0,35±0,07*

and OTM parameters on both A2780 and PC-3 cell lines ($p < 0.05$), compounds **1**–**4** and only **FSC-3** caused a genotoxic effect on LNCAP ($p < 0.05$). Genotoxicity results revealed that these substances are effective on DNA.

DNA damage studies of compounds **1**–**4** and **FSC 1**–**4** Compounds in human prostate cancer cell lines (LNCaP, PC-3) and human ovarian cancer (A2780) cell lines were performed at the highest concentration (100 μM). By determining the parameters of TL, TI, and OTM,

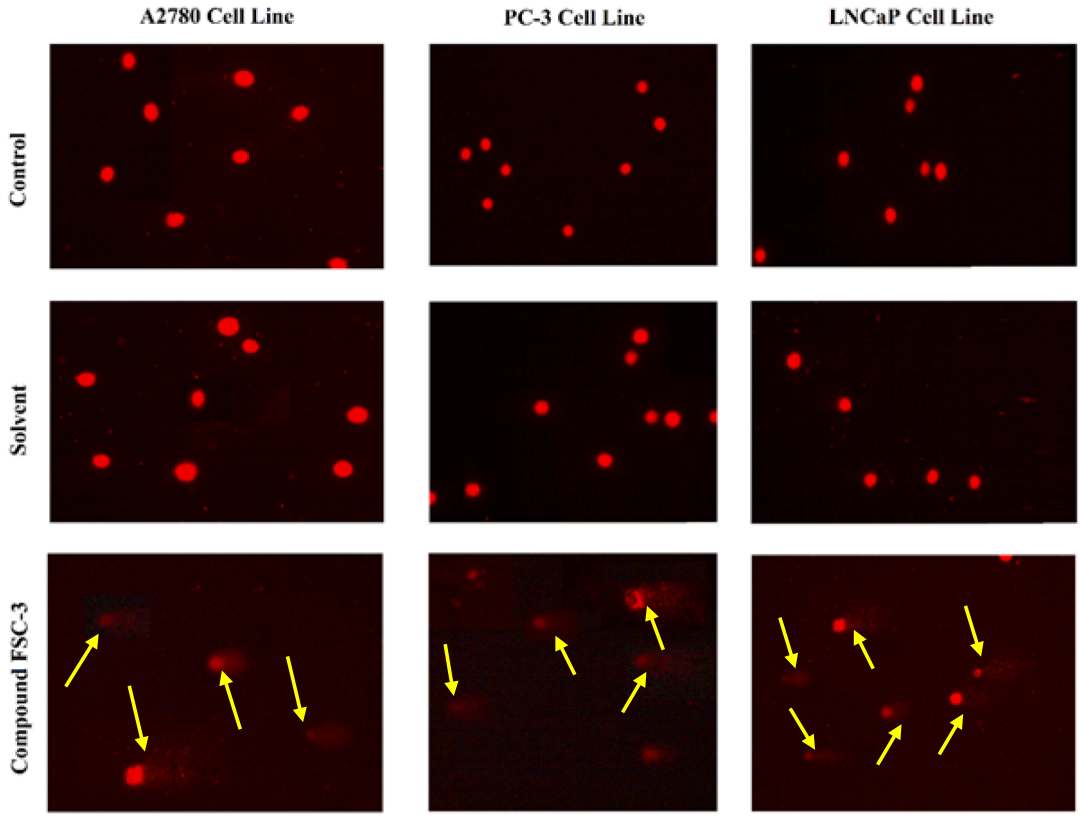

Fig. 7. Images obtained from three different cancer cells in which **FSC-3** compound was effective within the scope of Comet Assay trials (Yellow arrows indicate comet images showing DNA damage; x10). (For interpretation of the references to colour in this figure legend, the reader is referred to the web version of this article.)

parameters produced at a dose of 100 μM, the presence and rate of DNA damage were determined by the changes in these parameters in Table 1 and comet assay images are presented in Fig. 7.

Comet analysis results from DNA damage studies of compounds **1**–**4** and **FSC 1**–**4** compounds in human prostate cancer cell lines (LNCaP, PC-3) and human ovarian cancer (A2780) cell lines at the 100 μM dose TL, TI, and OTM parameters showed that changes were observed and these changes were statistically significant. As a result, it is understood that cell death proceeds through the mechanism of DNA damage.

2.3. Theoretical calculations

2.3.1. Molecular docking and ADMET studies

Molecular docking studies were performed to identify possible interactions of ligands **(1–4 and FSC 1–4)** with cancer-related enzymes and correlate them with in vitro results. Docking studies on Bcl-2, p53, Caspase-3, SRC-Kinase proteins, and DNA demonstrate that phosphazene derivatives **(FSC 1–4)** have higher binding scores than chalcone derivatives **(1–4)** due to the expansion of the surface areas of the molecules. Chalcone derivatives have similar binding scores at the active sites of all proteins but the highest ligand efficiency among them is for DNA and p53. Also, the binding scores for the phosphazene derivatives are almost similar, and the SRC-kinase protein has a high affinity for all final molecules. High binding affinities are given in Table 2 ranging from −10.0 to −12.0 kcal mol^{-1}. Although the large surface area of the molecules prevents the molecules from entering the active sites of the enzyme, the phosphazene structures are flexible and the substituents interacted easily with the active site due to several rotatable bonds it contains. Since the electropositive phosphazene ring can transfer its electrons to the substituents, the number of non-covalent interactions of electron-charged nucleophilic substituents with amino acids has been quite high. Several significant hydrogen bond interactions are present and pi-interactions also exist due to macrocyclic ligands (Fig. 8).

Table 2
Binding scores of **1**–**4** and **FSC1-4** on Bcl-2, Caspase-3, DNA, p53, and SRC-Kinase enzymes.

Compound	Bcl-2	Caspase-3	DNA	p53	SRC-Kinase
1	−4.64	−5.27	−6.14	−5.82	−5.58
2	−5.21	−5.46	−6.22	−6.00	−5.90
3	−5.75	−5.61	−6.76	−6.43	−6.49
4	−5.26	−5.40	−6.36	−6.33	−6.00
FSC-1	−8.55	−10.35	−8.97	−8.61	**−11.00**
FSC-2	**−10.57**	−10.18	−10.66	−10.68	−11.72
FSC-3	−8.90	−10.80	−11.34	**−10.23**	−11.48
FSC-4	−10.51	**−10.58**	−9.53	−9.48	−10.84

Overall, these findings in silico molecular docking studies are correlated with in vitro test results and these data are very useful for understanding experimental inhibition values. Repairing or damaging the DNA of a cancer cell will directly affect the cell and thus, it is very important to examine the interaction of molecules with DNA in cancer studies. The DNA binding scores of chalcone **(1–4)** and phosphazene-chalcone derivatives **(FSC 1–4)** are similar on Bcl-2, p53, Caspase-3, SRC-Kinase proteins. Due to the flexibility of the molecules, all of the ligands in chalcones and some of the substituents in phosphazene-chalcones are positioned in the minor groove region of DNA and interact with DNA bases (Fig. 9).

Fluorine group bearing chalcone-phosphazene with the highest score exhibited pi-cation, pi-anion, pi-lone pair, pi-pi stacking, and pi-alkyl interactions with the sugar-phosphate, thymine, guanine, and cytosine components of DNA. Considering the wide spectrum and interactions of ligands with DNA, these ligands are likely to have a repairing or damaging effect on the DNA of cancer cells. ADMET property results of

Table 3
Physicochemical drug properties of compounds **1**–**4** and **FSC 1**–**4**.

Properties	1	2	3	4	FSC1	FSC2	FSC3	FSC4
Mw	228.09	255.09	312.12	266.09	1497.42	1659.42	2001.57	1725.45
Volume	237.41	267.16	343.42	282.20	1465.59	1644.09	2101.66	1734.32
Density	0.961	0.955	0.909	0.943	1.022	1.009	0.952	0.995
nHA	4	4	2	3	27	27	15	21
nHD	1	1	1	1	0	0	0	0
nRot	3	4	3	3	30	36	30	30
nRing	2	2	4	3	13	13	25	19
MaxRing	6	6	13	9	6	6	13	9
nHet	4	4	2	3	30	30	18	24
fChar	0	0	0	0	0	0	0	0
nRig	13	14	23	18	84	90	144	114
Flexibility	0.231	0.29	0.13	0.17	0.36	0.40	0.21	0.26
TPSA	55.12	59.42	37.30	46.53	301.80	327.60	194.88	250.26
LogS	−3.267	−3.817	−5.691	−4.869	−4.079	−3.899	−9.692	−7.075
LogP	1.327	2.608	4.600	3.341	5.849	10.648	19.394	13.776
LogD	1.237	2.527	3.791	3.194	2.210	2.256	4.445	3.536

Mw = Molecular weight (Optimal: 100 ~ 600); **Volume** = Van der Waals volume; Density = Molecular weight/Volume; **nHA** = Number of hydrogen bond acceptors (Optimal: 0 ~ 12); **nHD** = Number of hydrogen bond donors (Optimal: 0 ~ 7); **nRot** = Number of rotatable bonds (Optimal: 0 ~ 11); **nRing** = Number of rings (Optimal: 0 ~ 6); **MaxRing** = Number of atoms in the biggest ring (Optimal: 0 ~ 18). **nHet** = Number of heteroatoms (Optimal:1 ~ 15); **fChar** = Formal charge (Optimal: −4 ~ 4); **nRig** = Number of rigid bonds (Optimal: 0 ~ 30); **Flexibility** = nRot/nRig; **TPSA** = Topological Polar Surface Area (Optimal: 0 ~ 140); **logS** = Log of the aqueous solubility (Optimal: −4 ~ 0.5 log mol/L); **logP** = Log of the octanol/water partition coefficient (Optimal: 0 ~ 3); **logD** = logP at physiological pH 7.4 (Optimal: 1 ~ 3).

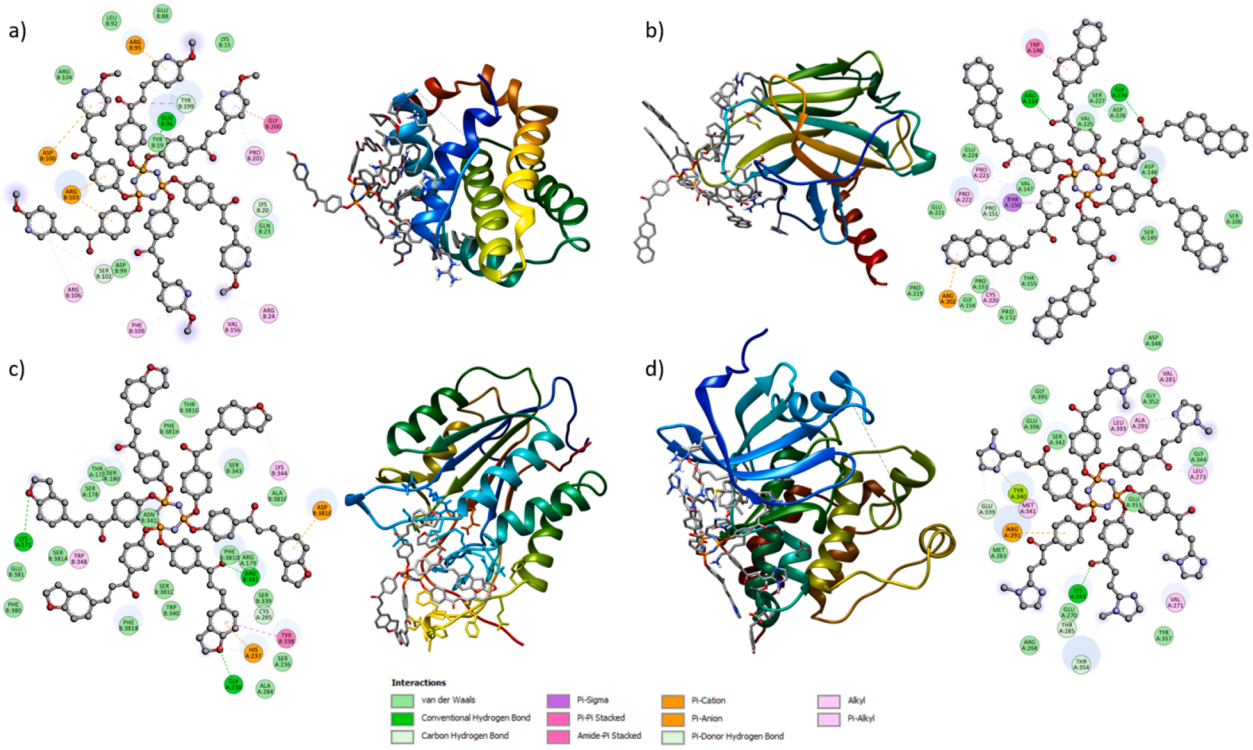

Fig. 8. 2D and 3D interactions of **FSC1-4** on active sites of Bcl-2 (a), p53 (b), Caspase-3 (c), and SRC-Kinase (d) enzymes.

drug candidate molecules indicate that phosphazene-chalcones (FSC 1–4) are slightly improbable from being drugs compared to chalcone derivatives with respect to optimal values physicochemically. On the other hand, chalcone derivatives (1–4) are in the range of optimal values for all physicochemical drug properties (Table 3).

The absorption properties show that the caco-2 permeability of the chalcone compounds is above the optimal value, acting as a p-glycoprotein inhibitor and substrate, while the caco-2 permeability of the phosphazene-chalcone compounds remains below the optimal value and acts only as a p-glycoprotein substrate. While chalcone derivatives are highly bound to plasma protein in their distribution properties, they partially pass through the blood–brain barrier. On the other hand, phosphazene chalcone derivatives can bind to plasma protein at a low rate, but cannot pass through the blood–brain barrier due to their large polar surface. In some diseases, the inability of the drug molecule to pass through the blood–brain barrier is considered an advantage because the BBB in the healthy brain prevents the passage of most compounds from the blood to the brain. In metabolism, compounds **FSC 1**–**4** are likely substrates of CYP2C9 and CYP2D6. Additionally, FSC-1 is an inhibitor of CYP2C9 and CYP3A4, but FSC4 is an inhibitor of CYP2C9. In contrast to phosphazene-chalcone derivatives in excretion, chalcone compounds have high clearance and a long half-life in the body. The carcinogenicity,

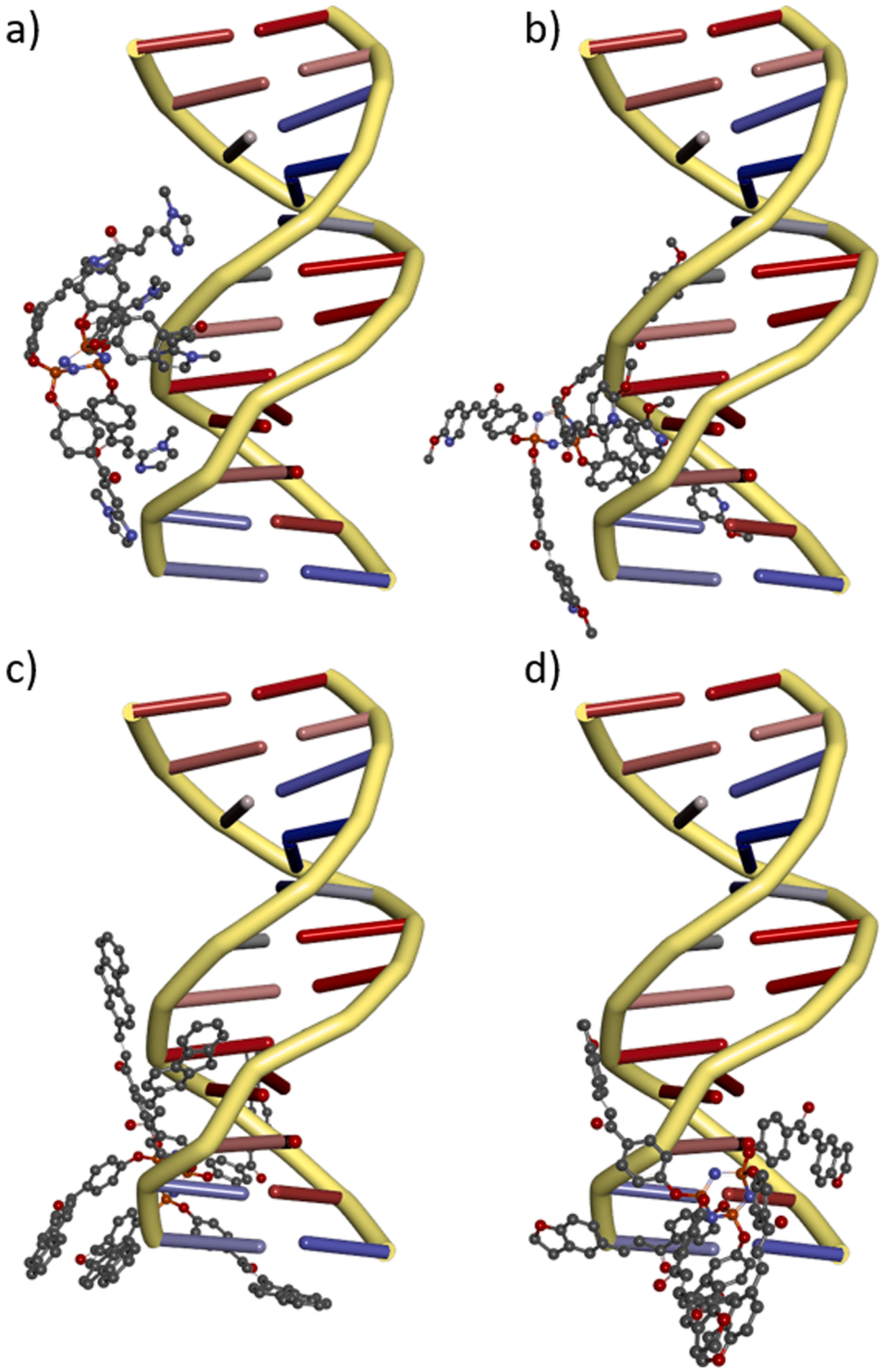

Fig. 9. Positions of the ligands FSC-1 (a), FSC-2 (b), FSC-3 (c), and FSC-4 (d) in the minor groove region of DNA.

hepatotoxicity, acute toxicity, genotoxicity, skin sensitization, and ames toxicity of all compounds were underestimated but warned against high doses in the liver.

3. Conclusion

Heterocyclic chalcone compounds and their new hexasubstituted phosphazene derivatives were successfully synthesized and the structures of the compounds were characterized. The synthesized four initials and four final compounds were tested against 3 different cancer cells at five different doses for cell viability. In the light of these tests, most of the compounds were effective on cell viability at high doses and the efficiency of cyclophosphazene compounds containing heterocyclic chalcones increased after chalcone addition. DNA damage analysis at the dose at which the compounds showed the best effect in the final step was performed by the comet assay method. These substances were applied at a dose of 100 μM on the cell lines and found that they were effective on the TL, TI, and OTM values of the cells and this effect was statistically significant ($p < 0.05$). Our study results have provided evidence that our newly synthesized heterocyclic chalcone compounds

and their *hexa*-substituted phosphazene derivatives have cytotoxic effects and exhibit cytotoxic effects by damaging DNA. The results suggest that both the organic subgroup and the cell type used in cancer research cause significant changes in the activity and that new studies will be designed on this subject and will add a new dimension to drug development studies.

4. Experimental procedures

4.1. Chemicals and instrumentation

4′-Hydroxyacetophenone, and hexachlorocyclotriphosphazene (trimer) were purchased from Alfa Aesar and the timer *n*-hexane was also used by recrystallization. The compounds 1-methyl-1H-imida zole-2-carbaldehyde, 6-methoxynicotinaldehyde, fluorene-2-carbox aldehyde, and 2,3-dihydrobenzofuran-5-carbaldehyde were purchased from Acros. Potassium carbonate and tetrahydrofuran were obtained from Merck, *n*-hexane, chloroform, sodium hydroxide, and ethyl alcohol from Sigma Aldrich. DMSO-d_6 and $CDCl_3$ used as a deuterated solvent for NMR studies were obtained from Merck.

A Bruker DPX 400 MHz spectrometer was used to measure ^{31}P, ^{1}H, and ^{13}C NMR spectra. The Thermo Scientific Nicolet iS5 FT-IR Spectrometer was used in the infrared analysis. Mass spectra of the compounds were recorded on Bruker Microflex LT MALDI-TOF MS spectrometer. The elemental analysis data were obtained using a LECO CHNS elemental analyzer. In cell culture studies, RPMI-1640 medium for cell types (Sigma-Aldrich, USA), Incubator with CO2 (Panasonic, Japan), trypsin-EDTA (Sigma-Aldrich, USA), Microplate reader (BioTEK Spectrophotometer), Inverted Microscope SOIF -XDS, Nuve Brand Autoclave (for sterilization) and biological safety cabinet (Nuve Brand MN-120) were used. An Isolab brand pH meter was used for pH measurements.

4.2. General synthesis and characterization of starting compounds (1–4)

The starting compounds were obtained pure by Claisen-Schmidt condensation [26]. The detailed synthesis procedure is given for compounds **1**–**4**. The ^{1}H, ^{13}C NMR and MS spectrum characterization spectra of all compounds were presented in Supplementary Information section.

4.2.1. Synthesis of compound 1

A 250 mL single neck reaction flask was added to 80 mL of ethyl alcohol and then 22.04 mmol 4′-hydroxy acetophenone was added and mixed until completely dissolved. Approximately 15 mL of 40% NaOH solution was added and it was mixed for 15 min. Finally, 22.48 mmol 1-methyl-1H-imidazole-2-carbaldehyde was added to the mixture and stirred at room temperature. The reaction was followed by thin-layer chromatography (approximate reaction time of 10 h, R_f (n-hexane: ethylacetate 5:3); 0.45;)). After the reaction was stopped, the solvent of the mixture was evaporated to 50 mL and precipitation in water. And then the pH was adjusted to 5–6. The precipitated yellow solid product was filtered off and washed with plenty of water and dried under vacuum. The solid was recrystallized from ethyl acetate to give the product a yellow crystal. Yield: 55; m.p: 78–79 °C; FT-IR (ATR, cm^{-1}): 3268 ν_{OH}, 3021, 3050 and 3062 $\nu_{C\text{-}H(Ar.)}$, 2928 $\nu_{C\text{-}H(Aliphatic)}$, 1651 $\nu_{C=O}$, 1518, 1578, 1596, 1603 and 1612 $\nu_{C=C}$. ^{1}H NMR (400 MHz, DMSO-d_6): δ = 3.83 (3H, s, H^{14}), 6.92–6.93 (2H, d, J = 8.4 Hz, $H^{3,5}$), 7.13 (1H, d, H^{12}), 7.39 (1H, d, H^{13}), 7.58–7.62 (1H, d, J = 15.0 Hz, H^{9}), 7.83–7.87 (1H, d, J = 15.0 Hz, H^{10}), 7.98–8.0 (2H, d, J = 8.8 Hz, $H^{2,6}$) and 10.51 (1H, s, H^{7}). ^{13}C-APT NMR (DMSO-d_6): δ = 129.47 C^{1}, 131.40 $C^{2,6}$, 116.02 $C^{3,5}$, 162.73 C^{4}, 187.14 C^{8}, 125.45 C^{9}, 130.18 C^{10}, 143.64 C^{11}, 128.31 C^{12}, 122.58 C^{13}, and 33.18 C^{14}. MALDI MS *m/z* Calcd. For $C_{13}H_{12}N_2O_2$ + (H^+): 229.25. Found: 229.187. Anal. Calcd. For $C_{13}H_{12}N_2O_2$, C, 68.41; H, 5.30; N, 12.27. Found: C, 68.46; H, 5.33; N, 12.31.

4.2.2. Synthesis of compound 2

22.04 mmol 4′-hydroxyacetophenone and 22.48 mmol 6-methoxynicotinaldehyde. R_f (n-hexane: ethylacetate 5:3); 0.45). Yield: 65%; m.p: 166–167 °C; FT-IR (ATR, cm^{-1}): 3290 ν_{OH}, 3045, and 3070 $\nu_{C\text{-}H(Ar.)}$, 2948 $\nu_{C\text{-}H(Aliphatic)}$, 1649 $\nu_{C=O}$, 1521, 1574, 1595, 1606 and 1614 $\nu_{C=C}$. ^{1}H NMR (400 MHz, DMSO-d_6): δ = 3.93 (3H, s, H^{16}), 6.88–6.95 (3H, m, $H^{3,5}$, and H^{14}), 7.67–7.71 (1H, d, J = 15.6 Hz, H^{9}), 7.87–7.92 (1H, d, J = 15.6 Hz, H^{10}), 8.07–8.09 (1H, d, J = 8.8 Hz, $H^{2,6}$), 8.35 (1H, s, H^{12}), 8.57 (1H, d, J = 7.6 Hz, H^{15}) and 10.41 (1H, s, H^{7}). ^{13}C-APT NMR (DMSO-d_6): δ = 129.54 C^{1}, 131.66 $C^{2,6}$, 115.83 $C^{3,5}$, 162.65 C^{4}, 187.29 C^{8}, 121.59 C^{9}, 139.84 C^{10}, 125.17 C^{11}, 149.72 C^{12}, 165.10 C^{13}, 111.57 C^{14}, 138.08 C^{15}, and 54.04 C^{16}. MALDI MS *m/z* Calcd. For $C_{15}H_{13}NO_3$ + (H^+): 256.27. Found: 256.153. Anal. Calcd. For $C_{15}H_{13}NO_3$, C, 70.58; H, 5.13; N, 5.49. Found: C, 70.61; H, 5.17; N, 5.53.

4.2.3. Synthesis of compound 3

22.04 mmol 4′-hydroxyacetophenone and 22.48 mmol fluorene-2-carboxaldehyde. R_f (n-hexane: ethylacetate 5:3); 0.44) Yield: 63%; m.p: 71–72 °C; FT-IR (ATR, cm^{-1}): 3216 ν_{OH}, 3030, and 3050 $\nu_{C\text{-}H(Ar.)}$, 2962 $\nu_{C\text{-}H(Aliphatic)}$, 1655 $\nu_{C=O}$, 1530, 1584, 1599, and 1610 $\nu_{C=C}$. ^{1}H NMR (400 MHz, DMSO-d_6): δ = 2.82 (2H, s, H^{17}), 6.75–6.77 (2H, d, J = 8 Hz, $H^{3,5}$), 7.07–7.11 (1H, d, J = 16 Hz, H^{9}), 7.25–7.29 (1H, d, J = 16 Hz, H^{10}), 7.48–7.59 (5H, m, $H^{12,16}$ and $H^{21\text{-}23}$), 7.81–7.83 (2H, d, H^{15}), 8.17–8.19 (2H, d, $H^{2,6}$), 8.72–8.76 (1H, d, H^{20}), and 10.16 (1H, s, H^{7}). ^{13}C NMR (DMSO-d_6): δ = 129.26 C^{1}, 131.68 $C^{2,6}$, 116.38 $C^{3,5}$, 161.14 C^{4}, 199.40 C^{8}, 125.32 C^{9}, 135.37 C^{10}, 129.19 C^{11}, 124.64 C12, 128.46 C^{13}, 131.14 C^{14}, 148.46 $C^{15,18}$, 127.54 C^{16}, 34.16 C^{17}, 131.05 C^{19}, 128.41 C^{20}, 126.13 C^{21}, 126.21 C^{22}, and 127.27 C^{23}. MALDI MS *m/z* Calcd. For $C_{22}H_{16}O_2$ + (H^+): 313.37. Found: 313.756. Anal. Calcd. For $C_{22}H_{16}O_2$, C, 84.59; H, 5.16. Found: C, 84.62; H, 5.19.

4.2.4. Synthesis of compound 4

22.04 mmol 4′-hydroxyacetophenone and 22.48 mmol 2,3-dihydrobenzofuran-5-carbaldehyde. R_f (n-hexane: ethylacetate 5:3); 0.42). Yield: 72%; m.p: 113–114 °C; FT-IR (ATR, cm^{-1}): 3260 ν_{OH}, 3040, and 3080 $\nu_{C\text{-}H(Ar.)}$, 2937 $\nu_{C\text{-}H(Aliphatic)}$, 1654 $\nu_{C=O}$, 1541, 1596, and 1606 $\nu_{C=C}$. ^{1}H NMR (400 MHz, DMSO-d_6): δ = 3.22–3.26 (2H, t, H^{17}), 4.60–4.64 (2H, t, H^{18}), 6.83–6.85 (1H, d, J = 8.4 Hz, H^{12}), 6.89–6.91 (2H, d, J = 8.8 Hz, $H^{3,5}$), 7.74–7.77 (1H, d, J = 8.0 Hz, H^{13}), 7.63–7.67 (1H, d, J = 15.2 Hz, H^{10}), 7.74–7.78 (1H, d, J = 15.2 Hz, H^{9}), 7.84 (1H, s, H^{16}), 8.05–8.08 (2H, d, J = 8.4 Hz, $H^{2,6}$), and 10.37 (1H, s, H^{7}). ^{13}C-APT NMR (DMSO-d_6): δ = 129.90 C^{1}, 131.66 $C^{2,6}$, 115.76 $C^{3,5}$, 162.41 C^{4}, 187.47 C^{8}, 119.31 C^{9}, 143.65 C^{10}, 128.12 C^{11}, 125.64 C^{12}, 128.96 $C^{13,14}$, 109.72 C^{15}, 131.45 C^{16}, 29.07 C^{17}, and 72.15 C^{18}. MALDI MS *m/z* Calcd. For $C_{17}H_{14}O_3$ + (H^+): 267.30. Found: 267.484. Anal. Calcd. For $C_{17}H_{14}O_3$, C, 76.68; H, 5.30. Found: C, 76.70; H, 5.35.

4.3. Synthesis of hexa-substituted cyclotriphosphazenes (FSC 1–4)

A similar method was applied in the synthesis of **FSC 1**–**4**. Therefore, the detailed procedure is specified only for the synthesis of compound **FSC-1**.

4.3.1. Synthesis of FSC-1

After the argon and airless reaction apparatus were prepared, 0.58 mmol **FSC** was added to the three-necked reaction flask containing 40 mL of dry acetone as solvent at 0 ^{0}C. And then 4.03 mmol K_2CO_3 was added to the mixture, which was dried overnight in the oven, and the reaction was stirred for 30 min. Finally, 1.74 mmol of compound **1** dissolved in 35 mL of acetone was added dropwise. The reaction was stirred for about one hour. Then the mixture was refluxed. The reaction was followed by thin-layer chromatography (The approximate reaction time is 8 h, R_f (n-hexane: ethyl acetate 5:4); 0.38)). After the reaction was stopped, the reaction was filtered. After evaporating some of the solvents, it was precipitated by adding 3% to 250 mL of NaOH solution. The solid product was filtered and washed copiously with water (until

pH 7). Finally, it was washed with ethyl alcohol and dried. The dried solid was dissolved in chloroform again and precipitated in *n*-hexane. Yield: 85%; white solid; m.p: 159–160 °C; FT-IR (KBr) ν_{max} (cm^{-1}): 3033 and 3071 $\nu_{Ar\text{-}CH}$, 2888 and 2961 $\nu_{Aliphatic\text{-}CH}$, 1661 $\nu_{C=O}$, 1501 and 1589 $\nu_{C=C}$, 1157 and 1179 $\nu_{P=N}$, 951 $\nu_{P\text{-}O\text{-}Ph}$. ^{31}P NMR (DMSO-$d_6$) δ = 8.10 (3P, s, PA, A3). ^{1}H NMR (DMSO-d_6, ppm) δ = 2.41 (3H, s, H^{14}, –CH_3), 7.10–7.12 (2H, d, J = 8.4 Hz, Ar-$H^{3,5}$), 7.32 (1H, d, J = 9.6 Hz, Ar-H^{12}), 7.36 (1H, Ar-H^{13}), 7.45–7.49 (1H, d, J = 15.6 Hz, H^{10} (–CH=), 7.64–7.69 (1H, d, J = 15.6 Hz, H^9 (=CH–)) and 7.91–7.93 (2H, d, J = 8.8 Hz, $H^{2,6}$ –Ar-H).^{13}C NMR (DMSO-d_6, ppm) δ = 131.54 C^1, 130.36 $C^{2,6}$, 120.75 C^3, 153.40 Ar-C^4, 129.44 C^5, 131.54 C^6, 188.81 C^8 (–C=O), 125.93 C^9, 135.66 C^{10}, 145.64 C^{11}, 128.78 C^{12}, 138.52 Ar-C^{13}, and 21.3 C^{14}. MALDI MS *m/z* Calcd. For $N_3P_3O_{12}C_{78}H_{66}N_{12}$ + (H^+): 1499.40. Found: 1499.231. Anal. Calcd. For $N_3P_3O_{12}C_{78}H_{66}N_{12}$, C, 62.52; H, 4.44; N, 14.02%; Found: C, 62.58; H, 4.49; N, 14.06%.

4.3.2. Synthesis of FSC-2

The procedure is similar to that of **FSC-1**, using **FSC** (0.58 mmol), compound **2** (1.74 mmol) and K_2CO_3 (4.03 mmol). R_f (n-hexane: ethyl acetate 5:4); 0.36). Yield: 82%; white solid; m.p: 194–195 °C; FT-IR (KBr) ν_{max} (cm^{-1}): 3068 $\nu_{Ar\text{-}CH}$, 2879 and 2968 $\nu_{Aliphatic\text{-}CH}$, 1663 $\nu_{C=O}$, 1500, 1577 and 1588 $\nu_{C=C}$, 1160 and 1181 $\nu_{P=N}$, 949 $\nu_{P\text{-}O\text{-}Ph}$. ^{31}P NMR (DMSO-$d_6$) δ = 8.25 (3P, s, PA, A3). ^{1}H NMR (DMSO-d_6, ppm) δ = 3.90 (3H, s, H^{16}, –OCH_3), 6.82–6.84 (1H, H^{14}), 7.14–7.16 (2H, $H^{3,5}$), 7.60–7.64 (1H, d, J = 15.6 Hz, H^{10}), 7.72–7.76 (1H, d, J = 15.6 Hz, H^9), 8.02–8.04 (2H, d, $H^{2,6}$), 8.22 (1H, s, H^{12}) and 8.43 (1H, s, H^{15}).^{13}C NMR (DMSO-d_6, ppm) δ = 135.39 C^1, 131.04 $C^{2,6}$, 111.49 $C^{3,5}$, 153.32 C^4, 187.69 C^8 (–C=O), 121.12 C^9, 141.42 C^{10}, 124.74 C^{11}, 149.76 C^{12}, 165.23 C^{13}, 120.74 $C^{14,}$ 138 C^{15}, and 54.01 C^{16}. MALDI MS *m/z* Calcd. For $N_3P_3O_{18}C_{90}H_{72}N_6$ + (H^+): 1661.53. Found: 1661.895. Anal. Calcd. For $N_3P_3O_{18}C_{90}H_{72}N_6$, C, 65.10; H, 4.37; N, 7.59%. Found: C, 65.14; H, 4.40; N, 7.63%.

4.3.3. Synthesis of FSC-3

The procedure is similar to that of **FSC-1**, using **FSC** (0.58 mmol), compound **3** (1.74 mmol) and K_2CO_3 (4.03 mmol). R_f (n-hexane: ethyl acetate 5:4); 0.39). Yield: 50%; white solid; m.p: 146–147 °C; FT-IR (KBr) ν_{max} (cm^{-1}): 3060 $\nu_{Ar\text{-}CH}$, 2889 and 2972 $\nu_{Aliphatic\text{-}CH}$, 1665 $\nu_{C=O}$, 1510, 1588 and 1601 $\nu_{C=C}$, 1162 and 1180 $\nu_{P=N}$, 953 $\nu_{P\text{-}O\text{-}Ph}$. ^{31}P NMR (DMSO-$d_6$) δ = 8.21 (3P, s, PA, A3). ^{1}H NMR (DMSO-d_6, ppm) δ = 3.89 (2H, H^{17}, –CH_2), 7.02–7.05 (1H, t, H^{23}), 7.10–7.12 (1H, d, J = 8.4 Hz, H^{12}), 7.22–7.25 (2H, d, J = 8.4. Hz, $H^{3,5}$), 7.30–7.49 (5H, m, H^{10}, Ar-$H^{15,16,\ 20,\ 22}$), 7.78–7.82 (1H, d, J = 15.6 Hz, H^9), and 7.95–8.06 (3H, m, $H^{2,6}$, H^{21}).^{13}C NMR (DMSO-d_6, ppm) δ = 130.4 C^1, 131.3 $C^{2,6}$, 117.2 $C^{3,5}$, 153.7 C^4, 188.3 C^8 (–C=O), 121.4 C^9, 135.5 C^{10}, 130.8 C^{11}, 122.1 C^{12}, 128.2 C^{13}, 160.1 $C^{14,}$ 136.4 C^{15}, 127.3 C^{16}, 55.8 C^{17}, 144.8 C^{18}, 147.4 C^{19}, 113.9 C^{21}, 122.4 C^{22}, 130.5 C^{23} and 121.9 C^{24}. MALDI MS *m/z* Calcd. For $N_3P_3O_{12}C_{132}H_{90}$ + (H^+): 2004.10. Found: 2004.224. Anal. Calcd. For $N_3P_3O_{12}C_{132}H_{90}$, C, 79.15; H, 4.53; N, 2.10%. Found: C, 79.19; H, 4.58; N, 2.17%.

4.3.4. Synthesis of FSC-4

The procedure is similar to that of **FSC-1**, using **FSC** (0.58 mmol), compound **4** (1.74 mmol) and K_2CO_3 (4.03 mmol). R_f (n-hexane: ethyl acetate 5:4); 0.37). Yield: 75%; white solid; m.p: 151–152 °C; FT-IR (KBr) ν_{max} (cm^{-1}): 3058 $\nu_{Ar\text{-}CH}$, 2838 and 2981 $\nu_{Aliphatic\text{-}CH}$, 1666 $\nu_{C=O}$, 1508, 1591 and 1604 $\nu_{C=C}$, 1161 and 1179 $\nu_{P=N}$, 951 $\nu_{P\text{-}O\text{-}Ph}$. ^{31}P NMR (DMSO-$d_6$) δ = 8.2 (3P, s, PA, A3). ^{1}H NMR (DMSO-d_6, ppm) δ = 3.22–3.26 (2H, t, H^{17}), 4.60–4.64 (2H, t, H^{18}), 6.83–6.85 (1H, d, H^{15}), 6.89–6.91 (2H, d, $H^{3,5}$), 7.63–7.67 (1H, d, H^9), 7.74–7.77 (1H, d, H^{10}), 7.84 (1H, s, H^{12}), and 8.05–8.08 (2H, $H^{2,6}$).^{13}C NMR (DMSO-d_6, ppm) δ = 129.90 C^1, 131.65 $C^{2,6}$, 115.76 $C^{3,5}$, 152.45 C^4, 187.41 C^8 (–C=O), 119.31 C^9, 143.66 C^{10}, 128.07 C^{11}, 125.64 C^{12}, 128.96 $C^{13,14}$, 109.72 $C^{15,}$ 131.45 C^{16}, 72.18 C^{18} and 29.12 C^{17}. MALDI MS *m/z* Calcd. For $N_3P_3O_{18}C_{102}H_{78}$ + (H^+): 1727.67. Found: 1727.706. Anal. Calcd. For $N_3P_3O_{18}C_{102}H_{78}$, C, 70.95; H, 4.55; N, 2.43%. Found: C, 71.00; H, 4.57; N, 2.47%.

4.4. Determination of in vitro cytotoxic activity with MTT assay

In this study, human prostate (LNCaP and PC-3) and ovarian cancer cell lines (A2780) were used as cell types. All cells were fed with RPMI-1640 medium (prepared by adding 10% FCS, 100U / mL penicillin and 0.1 mg / mL streptomycin) in 25 cm^2 culture flasks. In the incubator with carbon dioxide (5% CO_2), the media of the cells kept at 37 ^{0}C and in a humid environment were changed twice a week. When the cells were confluent they were removed from the flasks using the trypsin-EDTA solution and transferred to 96-well plates and used in 3-(4,5-dimethylthiazol-2-yl) -diphenyl tetrazolium bromide (MTT) assays [33,39]. Solutions of the substances in dimethylsulfoxide (DMSO) solvent was used in cell culture. For this reason, in the comparison of the results, the effects of the substances against DMSO were determined by statistical analysis. The toxic effect of DMSO on the cell was determined and although it had a toxic effect, it was found that it was not statistically significant. The same amount of solvent (DMSO) with concentrations of 1, 5, 25, 50, and 100 μM of the tested compounds **(1–4 and FSC 1–4)** was added to the wells containing the cells and in a CO_2 incubator (Panasonic / Japan). It was left to incubate at 37 ^{0}C for 24 h. After the incubations, the viability of the cells was determined using 0.4% tryphan blue in a hemocytometer.

The compliance of the groups to normal distribution was evaluated with the Kolmogorov Smirnov test. One-way analysis of variance was used to compare the groups. Homogeneity of variances was analyzed by the Levene test. After a one-way analysis of variance, it was observed that the variances were not homogeneous, and the TAMHANE T2 test was used for multiple comparisons. $p < 0.05$ was considered statistically significant. Data are expressed as mean ± standard error. $LogIC_{50}$ / IC_{50} values were calculated with Graphpad prism 6 computer program [34].

4.5. Determination of the genotoxicity with comet assay

Comet Assay, also known as single-cell gel electrophoresis, is widely used to determine DNA damage (genotoxicity) in many mammalian cell types such as lymphocytes [40], sperm cells [41], epithelial cells [42] and cancer cells [43]. In this study, the alkaline comet assay technique was used to determine DNA damage as described in our previous study [44] with minor modifications. Briefly, the microscope slides were precoated with 100 mL of 0.7% normal melting-point agarose in PBS and then dried in the dark at room temperature for one day. The cell viability was first assessed with the trypan blue exclusion test before starting the comet assay experiments. Analyzes were started when the percentage of viable cells was greater than 90%.

The cultured PC-3, A,2780, and LNCaP cells were incubated for 24 h with the highest concentration (100 μM) at which the compounds to be tested were effective. After the incubation, cell suspension was mixed with low melting agarose (LMA) at 37 ^{0}C and the cell suspension was pipetted and layered onto precoated slides. The slides were quickly covered with a coverslip and kept at 4 °C for 5 min to allow the agarose to solidify. After the coverslips were removed, slides were immersed in a freshly prepared cold neutral lysis solution (2.5 M NaCl, 100 mM EDTA, 10 mM Tris, pH > 10) with 1% Triton X-100 and 10% DMSO at 4 °C for 1 h.

Electrophoresis: After lysis, the slides were placed in a horizontal electrophoresis tank (Bio-Rad, USA), filled with cold neutral electrophoresis buffer. Electrophoresis was conducted at 25 V (0.83 V/cm) and 300 mA for 20 min. After electrophoresis, the slides were neutralized with neutralization buffer (0.4 M Tris, pH 7.5) 3 times at 4 °C for 5 min. Then the slides were dried and stained with 20 μg/ml ethidium bromide and covered with a coverslip. The slides were kept at 4 °C for 20 min before scoring. The entire process was conducted in the dark to prevent additional DNA damage.

Analysis of DNA damage: Twenty-five cells per slide and two slides

per sample were counted using a fluorescence microscope (Leica, Germany) equipped with suitable filters at 200 × magnification and the images recorded for offline analysis. The images were analyzed in Argenit Kameram software (Ankara, Turkey), and parameters of TI, TL, and OTM were determined to evaluate DNA damage for each substance. The data obtained from the comet assay were analyzed using one-way ANOVA, followed by post a location Tukey HSD test. All results were expressed as mean ± SEM or SD, and $p < 0.05$ was considered to be statistically significant.

4.6. Theoretical calculations

Autodock Vina [45] was used to determine the binding affinities and to see possible enzyme-substrate interactions in molecular docking study for compounds 1–4 and FSC 1–4. Compounds 1–4 and FSC 1–4 were prepared with MarvinSketch software, protonated, and their optimizations were performed by adding appropriate charges using MMFF94 Force Field parameters, which can be accessed in energy minimization protocols. For ligands 1–4 and FSC 1–4 tested in cancer cells, four potential proteins and one DNA involved in the cancer process were examined. B-cell lymphoma 2 (Bcl-2) protein is an important regulator of apoptosis and is known to promote oncogenesis. Caspases, like the Bcl-2 protein, play a key role in the apoptosis process [46]. These two proteins involved in the apoptotic process, are important targets for therapeutic intervention. Tp53 is a cancer suppressor enzyme that prevents genome degradation and alteration as well as mutations and ensures the stability of the genome. When DNA is damaged, DNA repair proteins are activated, but if the DNA cannot be repaired, apoptosis is triggered. Cancer that occurs, in this case, is possibly caused by a mutation in the Tp53 gene [47]. Cancer progression and metastasis are promoted by Src kinases. When Src activity increases, cancer cell proliferation accelerates, and intercellular adhesion decreases, thus increasing the potential for metastasis [48]. X-ray crystal structures of human B-cell lymphoma 2 (PDB code: 4LVT) [46], caspase-3 (PDB code: 1RE1) [49], deoxyribonucleic acid (PDB code: 1BNA) [50], protein 53 (PDB code: 5O1F) [47] and tyrosine SRC kinase (PDB code: 2BDF) [51] were retrieved from the Protein Data Bank (https://www.rcsb.org/). Water molecules were removed from the protein structures and polar hydrogens and Kollman charges [52] were added. Amino acids in the active site of the receptors were determined using Discovery Studio Visualizer 2021 v21.1.0.20298 [53]. Lamarckian Genetic Algorithm [54] was preferred as an insertion engine with all insertion parameters set to default. Inhibitors with the lowest energy insertion score were selected from among ten conformations provided by the Vina insertion calculations. Discovery Studio Visualizer 2021 v21.1.0.20298 and Chimera 1.13.1 programs were used to visualize 2D and 3D shapes.

Estimating the pharmacological properties of drug candidate molecules is a faster and more economical method and increases the probability of obtaining more accurate results. ADMET stands for absorption, distribution, metabolism, excretion, and toxicity. These criteria define the pharmaceutical activities of drug candidates. A free online web server, ADMETlab 2.0 (https://admetmesh.scbdd.com/) was used to estimate the properties of analyzed 1–4 and FSC 1–4 [55].

Declaration of Competing Interest

The authors declare that they have no known competing financial interests or personal relationships that could have appeared to influence the work reported in this paper.

Acknowledgement

This work was supported by Inonu University BAP (Grant number: TCD-2017-675).

Appendix A. Supplementary material

Supplementary data to this article can be found online at https://doi.org/10.1016/j.bioorg.2022.105997.

References

[1] M. Gleria, R. De Jaeger, Phosphazenes: A worldwide insight, Nova Publishers2004.
[2] H.R. Allcock, Recent advances in phosphazene (phosphonitrilic) chemistry, Chem. Rev. 72 (4) (1972) 315–356.
[3] K. Brandt, R. Kruszynski, T.J. Bartczak, I. Porwolik-Czomperlik, AIDS-related lymphoma screen results and molecular structure determination of a new crown ether bearing aziridinylcyclophosphazene, potentially capable of ion-regulated DNA cleavage action, Inorg. Chim. Acta 322 (1-2) (2001) 138–144.
[4] A. Binici, A. Okumuş, G. Elmas, Z. Kılıç, N. Ramazanoğlu, L. Açık, H. Şimşek, B. Çağdaş Tunalı, M. Türk, R. Güzel, T. Hökelek, Phosphorus–nitrogen compounds. Part 42. The comparative syntheses of 2-cis-4-ansa(N/O) and spiro(N/O) cyclotetraphosphazene derivatives: spectroscopic and crystallographic characterization, antituberculosis and cytotoxic activity studies, New J. Chem. 43 (18) (2019) 6856–6873.
[5] A. Okumuş, H. Akbaş, A. Karadağ, A. Aydın, Z. Kılıç, T. Hökelek, Antiproliferative Effects against A549, Hep3B and FL Cell Lines of Cyclotriphosphazene-Based Novel Protic Molten Salts: Spectroscopic, Crystallographic and Thermal Results, ChemistrySelect 2 (18) (2017) 4988–4999.
[6] S. Ture, C. Darcan, O. Türkyılmaz, Ö. Kaygusuz, Synthesis, structural characterization and antimicrobial activities of cyclochlorotriphosphazene derivatives derived from N-(1-Naphthyl) ethylenediamine, Phosphorus, Sulfur, and Silicon and the Related Elements 195 (6) (2020) 507–515.
[7] Ö. Işcan, R. Cemaloğlu, N. Asmafiliz, Z. Kiliç, L. Açik, P. Özbeden, T. Hökelek, Synthesis and spectroscopic properties of (N/O) mono-and dispirocyclotriphosphazene derivatives with benzyl pendant arms: study of biological activity, Turk. J. Chem. 44 (1) (2020) 15–30.
[8] G. Yakalı, A. Biçer, C. Eke, G.T. Cin, Solid state structural investigations of the bis (chalcone) compound with single crystal X-ray crystallography, DFT, gamma-ray spectroscopy and chemical spectroscopy methods, Radiat. Phys. Chem. 145 (2018) 89–96.
[9] J. Chen, L.e. Wang, Y.u. Fan, Y. Yang, M. Xu, X. Shi, Synthesis and anticancer activity of cyclotriphosphazenes functionalized with 4-methyl-7-hydroxycoumarin, New J. Chem. 43 (46) (2019) 18316–18321.
[10] E. Şenkuytu, P. Kızılkaya, Z. Ölçer, U. Pala, D. Davarcı, Y. Zorlu, H. Erdoğan, G. Yenilmez Çiftçi, Electrophoresis and biosensor-based DNA interaction analysis of the first paraben derivatives of spermine-bridged cyclotriphosphazenes, Inorg. Chem. 59 (4) (2020) 2288–2298.
[11] H. İbişoğlu, E. Erdemir, D. Atilla, Ş.Ş. Ün, S. Topçu, M.G. Şeker, Synthesis, characterization and antimicrobial properties of cyclotriphosphazenes bearing benzimidazolyl rings, Inorg. Chim. Acta 509 (2020), 119679.
[12] O. Ozay, M. Yildirim, H. Ozay, Synthesis, structural characterization, and anion interactions of new triazole-linked urea derivative fully substituted cyclotriphosphazene compounds, Phosphorus, Sulfur, and Silicon and the Related Elements 192 (3) (2017) 307–315.
[13] H. Baek, Y. Cho, C.O. Lee, Y.S. Sohn, Synthesis and antitumor activity of cyclotriphosphazene-(diamine) platinum (II) conjugates, Anticancer Drugs 11 (9) (2000) 715–725.
[14] B.R. Patil, S.S. Machakanur, R.S. Hunoor, D.S. Badiger, K.B. Gudasi, S.A. Bligh, Synthesis and anti-cancer evaluation of cyclotriphosphazene hydrazone derivatives, Der Pharma Chemica 3 (4) (2011) 377–388.
[15] J.Y. Yu, Y.J. Jun, S.H. Jang, H.J. Lee, Y.S. Sohn, Nanoparticulate platinum (II) anticancer drug: Synthesis and characterization of amphiphilic cyclotriphosphazene–platinum (II) conjugates, J. Inorg. Biochem. 101 (11–12) (2007) 1931–1936.
[16] A.N. Panche, A.D. Diwan, S.R. Chandra, Flavonoids: an overview, J. Nutr. Sci. 5 (2016), e47.
[17] C. Zhuang, W. Zhang, C. Sheng, W. Zhang, C. Xing, Z. Miao, Chalcone: A Privileged Structure in Medicinal Chemistry, Chem. Rev. 117 (12) (2017) 7762–7810.
[18] S. Ducki, The development of chalcones as promising anticancer agents, IDrugs : the Investigational Drugs J. 10(1) (2007) 42-6.
[19] S.N.A. Bukhari, M. Jasamai, I. Jantan, W. Ahmad, Review of Methods and Various Catalysts Used for Chalcone Synthesis, Mini-Rev. Org. Chem. 10 (1) (2013) 73–83.
[20] L. Sirka, H. Doğan, M.R. Bahar, E. Çalışkan, S. Tekin, H. Uslu, K. Koran, S. Sandal, A.O. Görgülü, (E)-1-(4-Hydroxyphenyl)-3-(substituted-phenyl)prop-2-en-1-ones: Synthesis, In Vitro Cytotoxic Activity and Molecular Docking Studies 69 (2022) 1–12.
[21] M. Wan, L. Xu, L.i. Hua, A. Li, S. Li, W. Lu, Y. Pang, C. Cao, X. Liu, P. Jiao, Synthesis and evaluation of novel isoxazolyl chalcones as potential anticancer agents, Bioorg. Chem. 54 (2014) 38–43.
[22] R. Arif, M. Rana, S. Yasmeen, M.S. Khan, M. Abid, M. Khan, Facile synthesis of chalcone derivatives as antibacterial agents: Synthesis, DNA binding, molecular docking, DFT and antioxidant studies, J. Mol. Struct. 1208 (2020), 127905.
[23] D. Coşkun, S. Tekin, S. Sandal, M.F. Coşkun, Synthesis, characterization, and anticancer activity of new benzofuran substituted chalcones, J. Chem. 2016 (2016) 1–8.
[24] F. Özen, A. Günel, A. Baran, DNA-binding, enzyme inhibition, and photochemical properties of chalcone-containing metallophthalocyanine compounds, Bioorg. Chem. 81 (2018) 71–78.

[25] C. Karthikeyan, N.S. Moorthy, S. Ramasamy, U. Vanam, E. Manivannan, D. Karunagaran, P. Trivedi, Advances in chalcones with anticancer activities, Recent Pat. Anti-Cancer Drug Discovery 10 (1) (2015) 97–115.
[26] B. Furniss, A. Hannaford, P. Smith, A. Tatchell, Vogel's textbook of practical organic chemistry, ELBS, Longman, London, 1989.
[27] L. Wang, Y.-X. Yang, X. Shi, S. Mignani, A.-M. Caminade, J.-P. Majoral, Cyclotriphosphazene core-based dendrimers for biomedical applications: An update on recent advances, J. Mater. Chem. B 6 (6) (2018) 884–895.
[28] M.F. Bobrov, M.I. Buzin, P.V. Primakov, E.M. Chistyakov, Investigation of hexakis [2-formylphenoxy] cyclotriphosphazene structure by single crystal X-ray diffraction and computer simulation, J. Mol. Struct. 1208 (2020), 127896.
[29] X. Su, L. Wang, J. Xie, X. Liu, H. Tomás, Cyclotriphosphazene-based derivatives for antibacterial applications: an update on recent advances, Curr. Org. Chem. 25 (2) (2021) 301–314.
[30] Y. Tümer, N. Asmafiliz, C.T. Zeyrek, Z. Kılıç, L. Açık, S.P. Çelik, M. Türk, B. Ç. Tunalı, H. Ünver, T. Hökelek, Syntheses, spectroscopic and crystallographic characterizations of cis-and trans-dispirocyclic ferrocenylphosphazenes: molecular dockings, cytotoxic and antimicrobial activities, New J. Chem. 42 (3) (2018) 1740–1756.
[31] G.Y. Çiftçi, N. Bayık, E.T. Eçik, E. Şenkuytu, M. Akşahin, T. Yıldırım, Synthesis of the first 2-hydroxyanthraquinone substituted cyclotriphosphazenes and their cytotoxic properties, New J. Chem. 44 (39) (2020) 16733–16740.
[32] A.O. Görgülü, K. Koran, F. Özen, S. Tekin, S. Sandal, Synthesis, structural characterization and anti-carcinogenic activity of new cyclotriphosphazenes containing dioxybiphenyl and chalcone groups, J. Mol. Struct. 1087 (2015) 1–10.
[33] K. Koran, Ç. Tekin, F. Biryan, S. Tekin, S. Sandal, A.O. Görgülü, Synthesis, structural and thermal characterizations, dielectric properties and in vitro cytotoxic activities of new 2, 2, 4, 4-tetra (4′-oxy-substituted-chalcone)-6, 6-diphenylcyclotriphosphazene derivatives, Med. Chem. Res. 26 (5) (2017) 962–974.
[34] K. Koran, Ç. Tekin, E. Çalışkan, S. Tekin, S. Sandal, A.O. Görgülü, Synthesis, structural and thermal characterizations and in vitro cytotoxic activities of new cyclotriphosphazene derivatives, Phosphorus, Sulfur, and Silicon and the Related Elements 192 (9) (2017) 1002–1011.
[35] H. Akbaş, A. Okumuş, Z. Kılıç, T. Hökelek, Y. Süzen, L.Y. Koç, L. Açık, Z.B. Celik, Phosphorus-nitrogen compounds part 27. Syntheses, structural characterizations, antimicrobial and cytotoxic activities, and DNA interactions of new phosphazenes bearing secondary amino and pendant (4-fluorobenzyl)spiro groups, Eur. J. Med. Chem. 70 (2013) 294–307.
[36] S.D. Durgapal, R. Soni, S. Umar, B. Suresh, S.S. Soman, 3-Aminomethyl pyridine chalcone derivatives: Design, synthesis, DNA binding and cytotoxic studies, Chem. Biol. Drug Des. 92 (1) (2018) 1279–1287.
[37] I. Beria, P.G. Baraldi, P. Cozzi, M. Caldarelli, C. Geroni, S. Marchini, N. Mongelli, R. Romagnoli, Cytotoxic α-Halogenoacrylic Derivatives of Distamycin A and Congeners, J. Med. Chem. 47 (10) (2004) 2611–2623.
[38] M. Işıklan, N. Asmafiliz, E.E. Ozalp, E.E. Ilter, Z. Kılıç, B.n. Çoşut, S. Yesilot, A. Kılıç, A. Öztürk, T. Hokelek, Phosphorus− nitrogen compounds. 21. syntheses, structural investigations, biological activities, and DNA interactions of new N/O spirocyclic phosphazene derivatives. The NMR behaviors of chiral phosphazenes with stereogenic centers upon the addition of chiral solvating agents, Inorganic Chem. 49(15) (2010) 7057-7071.
[39] F. Denizot, R. Lang, Rapid colorimetric assay for cell growth and survival. Modifications to the tetrazolium dye procedure giving improved sensitivity and reliability, J. Immunological Methods 89(2) (1986) 271-7.
[40] S. Sandal, B. Yilmaz, Genotoxic effects of chlorpyrifos, cypermethrin, endosulfan and 2, 4-D on human peripheral lymphocytes cultured from smokers and nonsmokers, Environ. Toxicol. 26 (5) (2011) 433–442.
[41] N. Tug, S. Sandal, B. Ozelgun, B. Yilmaz, Correlation of spermiogram profiles with DNA damage in sperm cells of infertile men: a comet assay study, Gynecol. Endocrinol. 27 (1) (2011) 49–54.
[42] K. Sarıca, H. Aydin, F. Yencilek, D. Telci, B. Yilmaz, Human umbilical vein endothelial cells accelerate oxalate-induced apoptosis of human renal proximal tubule epithelial cells in co-culture system which is prevented by pyrrolidine dithiocarbamate, Urol. Res. 40 (5) (2012) 461–466.
[43] M. Cheki, A. Shirazi, A. Mahmoudzadeh, J.T. Bazzaz, S.J. Hosseinimehr, The radioprotective effect of metformin against cytotoxicity and genotoxicity induced by ionizing radiation in cultured human blood lymphocytes, Mutation Res./Genetic Toxicol. Environ. Mutagenesis 809 (2016) 24–32.
[44] S. Sandal, B. Yilmaz, D.O. Carpenter, Genotoxic effects of PCB 52 and PCB 77 on cultured human peripheral lymphocytes, Mutation Res./Genetic Toxicol. Environ. Mutagenesis 654 (1) (2008) 88–92.
[45] O. Trott, A.J. Olson, AutoDock Vina: improving the speed and accuracy of docking with a new scoring function, efficient optimization, and multithreading, J. Comput. Chem. 31 (2) (2010) 455–461.
[46] A.J. Souers, J.D. Leverson, E.R. Boghaert, S.L. Ackler, N.D. Catron, J. Chen, B. D. Dayton, H. Ding, S.H. Enschede, W.J. Fairbrother, D.C.S. Huang, S.G. Hymowitz, S. Jin, S.L. Khaw, P.J. Kovar, L.T. Lam, J. Lee, H.L. Maecker, K.C. Marsh, K. D. Mason, M.J. Mitten, P.M. Nimmer, A. Oleksijew, C.H. Park, C.-M. Park, D. C. Phillips, A.W. Roberts, D. Sampath, J.F. Seymour, M.L. Smith, G.M. Sullivan, S. K. Tahir, C. Tse, M.D. Wendt, Y. Xiao, J.C. Xue, H. Zhang, R.A. Humerickhouse, S. H. Rosenberg, S.W. Elmore, ABT-199, a potent and selective BCL-2 inhibitor, achieves antitumor activity while sparing platelets, Nat. Med. 19 (2) (2013) 202–208.
[47] M.G.J. Baud, M.R. Bauer, L. Verduci, F.A. Dingler, K.J. Patel, D. Horil Roy, A. C. Joerger, A.R. Fersht, Aminobenzothiazole derivatives stabilize the thermolabile p53 cancer mutant Y220C and show anticancer activity in p53–Y220C cell lines, Eur. J. Med. Chem. 152 (2018) 101–114.
[48] R.B. Irby, T.J. Yeatman, Role of Src expression and activation in human cancer, Oncogene 19 (49) (2000) 5636–5642.
[49] J.W. Becker, J. Rotonda, S.M. Soisson, R. Aspiotis, C. Bayly, S. Francoeur, M. Gallant, M. Garcia-Calvo, A. Giroux, E. Grimm, Y. Han, D. McKay, D. W. Nicholson, E. Peterson, J. Renaud, S. Roy, N. Thornberry, R. Zamboni, Reducing the Peptidyl Features of Caspase-3 Inhibitors: A Structural Analysis, J. Med. Chem. 47 (10) (2004) 2466–2474.
[50] H.R. Drew, R.M. Wing, T. Takano, C. Broka, S. Tanaka, K. Itakura, R.E. Dickerson, Structure of a B-DNA dodecamer: conformation and dynamics, Proc. Natl. Acad. Sci. 78 (4) (1981) 2179–2183.
[51] D. Dalgarno, T. Stehle, S. Narula, P. Schelling, M. Rose van Schravendijk, S. Adams, L. Andrade, J. Keats, M. Ram, L. Jin, T. Grossman, I. MacNeil, C. Metcalf III, W. Shakespeare, Y. Wang, T. Keenan, R. Sundaramoorthi, R. Bohacek, M. Weigele, T. Sawyer, Structural Basis of Src Tyrosine Kinase Inhibition with a New Class of Potent and Selective Trisubstituted Purine-based Compounds, Chem. Biol. Drug Des. 67 (1) (2006) 46–57.
[52] U.C. Singh, P.A. Kollman, An approach to computing electrostatic charges for molecules, J. Comput. Chem. 5 (2) (1984) 129–145.
[53] D.S. Biovia, Discovery Studio Visualizer, Dassault Systèmes San Diego, CA, USA, 2021.
[54] G.M. Morris, D.S. Goodsell, R.S. Halliday, R. Huey, W.E. Hart, R.K. Belew, A. J. Olson, Automated docking using a Lamarckian genetic algorithm and an empirical binding free energy function, J. Comput. Chem. 19 (14) (1998) 1639–1662.
[55] G. Xiong, Z. Wu, J. Yi, L. Fu, Z. Yang, C. Hsieh, M. Yin, X. Zeng, C. Wu, A. Lu, X. Chen, T. Hou, D. Cao, ADMETlab 2.0: an integrated online platform for accurate and comprehensive predictions of ADMET properties, Nucleic Acids Res. 49 (W1) (2021) W5–W14.